# A High-Order Implicit Finite Element Method for Integrating the Extended-Magneto-Hydrodynamic Equations in Two Dimensions

**S. C. Jardin, J. Breslau, and N. Ferraro**
**January 8, 2007**

*Plasma Physics Laboratory, Princeton University, P.O. Box 451, Princeton, NJ 08543-451*

## Abstract

We describe a new method for solving the time-dependent extended-magnetohydrodynamic (X-MHD) equations in two dimensions that has significant advantages over other methods. The stream-function/potential representation of the velocity and magnetic field vectors, while fully general, allows accurate description of nearly incompressible fluid motions and manifestly satisfies the divergence condition on the magnetic field. Through analytic manipulation, the split semi-implicit method breaks the full matrix time advance into four sequential time advances, each involving smaller matrices. The use of a high order triangular element with continuous first derivatives ($C^1$ continuity) allows the Galerkin method to be applied without introduction of new auxiliary variables (such as the vorticity or the current density). These features, along with the manifestly compact nature of the fully node-based $C^1$ finite elements, lead to minimum size matrices for an unconditionally stable method with order of accuracy $h^4$. The resulting matrices are compatible with direct factorization using SuperLU_dist. We demonstrate the accuracy of the method by presenting examples of two-fluid linear wave propagation, two-fluid linear eigenmodes of a tilting cylinder, and of a challenging nonlinear problem in two-fluid magnetic reconnection.

E-mail address: jardin@pppl.gov

## I. Introduction:

It is well known that the "two-fluid" or Extended Magnetohydrodynamic (X-MHD) equations for a magnetized plasma present many numerical challenges. Even in the simpler ideal MHD model, a symmetric hyperbolic system which is a subset of the X-MHD equations, there are three distinct wave types with a wide separation of propagation speeds and with complex polarizations when applied to magnetized plasma conditions typical of fusion plasmas. When discretized on a finite difference or finite element mesh, these alone lead to a range of timescales and accuracy requirements that are a challenge to address with a single simulation. [1]

The full X-MHD equations compound this difficulty by introducing new terms which add dissipative phenomena and wave dispersion into the system [2]. Fully explicit solution techniques are generally not practical except for simulating the fastest timescale phenomena, which is of limited interest. To address the slower timescales, an implicit method is required, and the multiple-timescales and differing polarizations then manifest themselves as one or more poorly conditioned matrix equations that need to be solved to advance the solution from one timestep to the next. These matrices are either calculated analytically [3-5] (as in this paper) or are formed numerically as part of a nonlinear Newton method. [6-8]

It has been shown that in two dimensions (2D), a particular *18* degree-of-freedom polynomial triangular finite element with $C^1$ continuity, sometimes called the "reduced quintic" or $Q_{18}$, offers some unique advantages over other representations.[9-11] This element represents each scalar field in each triangular element as a quintic polynomial, which would normally require *21* coefficients. Of these, *18* are determined by the data (*6* values of the function and its first and second derivatives at each of the *3* nodes) and the other *3* by the requirement that the normal derivative along each edge be a cubic polynomial in the edge length, from which the $C^1$ property follows. The resulting representation contains a complete quartic polynomial, and thus has leading error of order $h^5$. It is also fully bivariate, and thus free of the directional bias that a tensor product representation would introduce.

The $Q_{18}$ element has the fewest number of degrees of freedom (DOF) compared to other finite elements representations with the same asymptotic error, and thus leads to implicit matrix equations of minimum rank [3]. This follows from the fact that all the DOF are defined at the nodes, and are thus shared by all the surrounding triangular elements. Also, the $C^1$ continuity property allows these elements to be applied directly to equations with spatial derivatives of up to $4^{th}$ order by using the Galerkin method and shifting two of the derivatives to the trial function by integration by parts. This makes feasible the numerical solution of the X-MHD equations in their stream function/potential form, which has many advantages over solving the primitive form of the equations, especially when a strong background magnetic field is present.

The work presented here is a continuation and generalization of Appendix D of Reference [3]. In that work, a method was presented for the 2-field reduced MHD equations in 2D slab geometry. This has subsequently been generalized to the 4-field Fitzpatrick-Porcelli equations [4]. In the present work, we generalize these equations to the "complete" 8-field 2-

fluid model, but continue to restrict the geometry to 2D slab geometry. One feature of this formulation is that the previous 2-field and 4-field models will be seen to be non-trivial subsets of the more complete model presented here. This allows direct comparison with and evaluation of the assumptions made in developing the reduced models.


## I. The Equations

Consider the set of X-MHD equations for the evolution of the plasma number density, the mass-flow velocity, the ion pressure, the electron pressure and the magnetic field, and the definitions of the electric field and the electrical current density (in SI units):

$$\frac{\partial n}{\partial t} + \nabla \cdot (n\vec{V}) = 0 \tag{2.1a}$$

$$nM_i(\frac{\partial \vec{V}}{\partial t} + \vec{V} \cdot \nabla \vec{V}) + \nabla p = \vec{J} \times \vec{B} + M_i n\vec{g} - \nabla \cdot \ddot{\Pi}_i \tag{2.1b}$$

$$\frac{1}{(\gamma - 1)}\left[\frac{\partial p_i}{\partial t} + \nabla \cdot \left(p_i \vec{V}\right)\right] = -p_i \nabla \cdot \vec{V} - \Pi_i : \nabla V - \nabla \cdot \vec{q}_i - Q_\Delta \tag{2.1c}$$

$$\frac{1}{(\gamma - 1)}\left[\frac{\partial p_e}{\partial t} + \nabla \cdot \left(p_e \vec{V}\right)\right] = -p_e \nabla \cdot \vec{V} + \frac{\vec{J}}{ne} \cdot \left[\frac{n^\gamma}{(\gamma - 1)}\nabla\left(p_e / n^\gamma\right) + \vec{R}\right]$$

$$+ \nabla\left(\frac{\vec{J}}{ne}\right) : \ddot{\Pi}_e - \nabla \cdot \vec{q}_e + Q_\Delta \tag{2.1d}$$

$$\frac{\partial \vec{B}}{\partial t} = -\nabla \times \vec{E} \tag{2.1e}$$

$$\vec{E} + \vec{V} \times \vec{B} = \frac{1}{ne}\left(\vec{R} + \vec{J} \times \vec{B} - \nabla p_e - \nabla \cdot \ddot{\Pi}_e\right) \tag{2.1f}$$

$$\mu_0 \vec{J} = \nabla \times \vec{B} \tag{2.1g}$$

Here, the random heat flux vectors for the ions and electrons are denoted $\vec{q}_i$ and $\vec{q}_e$, the equipartition term is denoted $Q_\Delta \equiv 3m_e(p - 2p_e)/(M_i \tau_e)$, and we have introduced the ratio of specific heats, $\gamma$, which has the classical value of $\gamma$=5/3. The electron-ion momentum transfer term is taken here to have the simplified form proportional to the plasma current; $\vec{R} = \eta ne\vec{J}$ although future studies will use the more correct form $\vec{R} = \eta ne\left(\vec{J} + \frac{3e}{5T_e}\vec{q}_e\right)$. A gravitational force $\vec{g} \equiv -g\hat{y}$ has been included, where g is a constant. The last two equations imply that the total fluid pressure, denoted by $p \equiv p_e + p_i$, obeys the equation:

$$\frac{1}{(\gamma - 1)}\left[\frac{\partial p}{\partial t} + \nabla \cdot \left(p\vec{V}\right)\right] = -p\nabla \cdot \vec{V} - \Pi_i : \nabla V - \nabla \cdot (\vec{q}_i + \vec{q}_e) \tag{2.2}$$

$$+ \frac{\vec{J}}{ne} \cdot \left[\frac{n^\gamma}{(\gamma - 1)}\nabla\left(p_e / n^\gamma\right) + \vec{R}\right] + \nabla\left(\frac{\vec{J}}{ne}\right) : \ddot{\Pi}_e$$

These equations have the energy integral:

$$\frac{\partial}{\partial t}\left[\frac{1}{2\mu_0}B^2 + \frac{1}{2\mu_0}nM_iV^2 + \frac{p}{(\gamma-1)}\right]$$

$$= -\nabla\bullet\left[\frac{\gamma}{(\gamma-1)}\left(p\vec{V} - \frac{p_e\vec{J}}{en}\right) + \vec{E}\times\vec{B} + \ddot{\Pi}_i\cdot\vec{V} - \frac{1}{ne}\ddot{\Pi}_e\cdot\vec{J} + \tfrac{1}{2}nM_iV^2\vec{V} + \vec{q}_e + \vec{q}_i\right]$$

$$+ M_i n\vec{V}\bullet\vec{g}$$

(2.3)

This implies conservation of energy if the gravitational potential is absent and the flux terms on the right vanish everywhere on the computational boundary.

The ion viscous stress term is taken to have the form:

$$\ddot{\Pi}_i = -\mu\left[\nabla\vec{V} + \nabla\vec{V}^\dagger\right] - 2(\mu_C - \mu)\left(\nabla\bullet\vec{V}\right)\vec{I} + \ddot{\Pi}_i^{GV}$$

$$\nabla\bullet\ddot{\Pi}_i = -\mu\nabla^2\vec{V} - (2\mu_C - \mu)\nabla\left(\nabla\bullet\vec{V}\right) + \nabla\bullet\ddot{\Pi}_i^{GV}$$

(2.4)

Here $\mu$ and $\mu_C$ are the incompressible and compressible coefficients of viscosity that satisfy the positivity constraints $\mu > 0$ and $\mu_C > (2/3)\mu$. [12] In the present work, we are not including the gyroviscous contribution (the rightmost term) in equation (2.4) in either the formulation or the examples. The inclusion of this term is discussed in [13].

We take the electron stress tensor to have the form of a hyper-resistivity, with coefficient $\lambda$.:

$$\ddot{\Pi}_e = \lambda\eta ne\nabla\vec{J}$$

(2.5)

The heat flux terms are expressed in terms of the isotropic and parallel heat flux coefficients $\kappa^e$, $\kappa$, $\kappa_\parallel^e$, and $\kappa_\parallel$. They have the following form:

$$\vec{q} = -\kappa\nabla T - \kappa_\parallel\nabla_\parallel T$$

$$\vec{q}_e = -\kappa^e\nabla T_e - \kappa_\parallel^e\nabla_\parallel T_e$$

(2.6)

The incorporation of the parallel heat flux terms is discussed in [3] and for that reason will not be repeated in the formulation presented here. The temperatures are defined in terms of the pressures and densities as

$$T_e = \frac{p_e}{k_B n}, \quad T = \frac{p}{k_B n},$$

(2.7)

In the remainder of the paper we adopt the normalized form of the equations. The normalization amounts to adopting a standard density and magnetic field strength $n_0$ and $B_0$. All lengths, velocities, and pressures are then scaled to the ion skin depth, the Alfven velocity, and the magnetic pressure in the usual way:

$$l_0 \equiv \frac{c}{\omega_{pi}} = \left[\frac{M_i}{n_0 e^2 \mu_0}\right]^{1/2}$$

$$V_0 \equiv \frac{B_0}{\sqrt{\mu_0 M_i n_0}} \tag{2.8}$$

$$p_0 = \frac{B_0^2}{\mu_0}$$

Other scaled quantities can be derived from these using dimensional relations. For example the time is scaled to $t_0 = l_0 / V_0$, etc.

## III. The Numerical representation

In 2D (x,y plane), without loss of generality, we represent the fluid velocity and magnetic field in terms of the five scalar variables $U(x, y, t), \chi(x, y, t), V_z(x, y, t), \psi(x, y, t), I(x, y, t)$ as follows:

$$\vec{V} = \nabla U \times \hat{z} + \nabla \chi + V_z \hat{z}, \tag{3.1}$$

$$\vec{B} = \nabla \psi \times \hat{z} + I \hat{z}$$

This representation, which is the Cartesian limit of that used in the M3D code [14], effectively separates incompressible and compressible motions in order to minimize spectral pollution [1]. Also, the form for the magnetic field is intrinsically divergence-free and involves only two scalar variables.

Each of the scalar variables is expanded in a set of polynomial triangular finite elements. At each node, there are *6* degrees of freedom (DOF) for each scalar, corresponding to the value of the function and its *2* first and *3* second derivatives at that node. Basis functions $v_i(x, y)$ are chosen that are piecewise quintic with the property that the function and its first derivative are continuous across element boundaries. Each basis function has the value of unity for one of the six DOF for that function at one node, with the property that the basis function and its two first and three second derivatives vanish at all the surrounding nodes as described in [3].

Within each triangular finite element, the solution is expressed as the sum of the product of the *18* time-independent spatial basis functions for that element (*6* from each of the three nodes) times the time-dependent amplitudes. Thus, for example, at time $t = t^n$, the velocity stream function in a particular triangular element is represented as:

$$U(x, y, t^n) = \sum_{j=1}^{18} v_j U_j^n \tag{3.2}$$

In a similar way, the other 7 scalar fields $\chi, V_z, \psi, I, n, p, p_e$ at time $t^n$ are represented by the amplitudes: $X_j^n, V_{zj}^n, \Psi_j^n, I_j^n, N_j^n, P_j^n, P_{ej}^n$. To derive the discrete form of the velocity advance

equations, we first operate on the momentum equation (2.1b) with the three annihilation operators

$$-\hat{z}\cdot\nabla\times$$
$$\hat{z}\cdot$$
$$\nabla\bullet$$
(3.3)

These have the effect of removing the compressible motion from the first equation, and the incompressible motion from the third. To form the weak form of the equations as required by the Galerkin method, each equation is then multiplied by each basis function $v_i(x,y)$ (6 for each node for each scalar variable) and then integrated over the domain. Integration by parts converts the three annihilation operators in (3.3) to the vector projections:

$$\hat{z}\cdot\nabla v_i\times$$
$$v_i\hat{z}\cdot$$
$$-\nabla v_i\bullet$$
(3.3)'

Straightforward manipulation, neglecting terms involving spatial derivatives of the viscosities and of the density multiplying the viscosities, and using Stokes and Gauss's theorems to convert total derivatives to boundary terms that vanish, yields the following integrands for the weak form of the three scalar momentum equations:

$$-n\left(v_i,\dot{U}\right)+n\left[v_i,\dot{\chi}\right]-n\nabla^2 U\left[v_i,U\right]+\tfrac{1}{2}n\left[v_i,(U,U)\right]-n\nabla^2 U\left(v_i,\chi\right)$$
$$+\left[n,v_i\right]\left[\chi,U\right]+\tfrac{1}{2}n\left[v_i,(\chi,\chi)\right]+\nabla^2\psi\left[v_i,\psi\right]-gv_i n_x-\mu\nabla^2 v_i\nabla^2 U=0$$
(3.4)

$$v_i n\dot{V}_z+v_i n\left[V_z,U\right]+v_i n\left(V_z,\chi\right)+\mu\nabla v_i\bullet\nabla V_z+v_i\left[\psi,I\right]=0$$
(3.5)

$$-n\left[v_i,\dot{U}\right]-n\left(v_i,\dot{\chi}\right)+n\nabla^2 U\left(v_i,U\right)-\tfrac{1}{2}n\left(v_i,(U,U)\right)-n\nabla^2 U\left[v_i,\chi\right]$$
$$-n\left(v_i,[\chi,U]\right)-\tfrac{1}{2}n\left(v_i,(\chi,\chi)\right)-\nabla^2\psi\left(v_i,\psi\right)+gv_i n_y-2\mu_C\nabla^2 v_i\nabla^2\chi$$
$$-I\left(v_i,I\right)-\left(v_i,p\right)=0$$
(3.6)

Here and elsewhere we use the notation that for any two scalar quantities $a$ and $b$, we define the Poisson bracket: $[a,b]\equiv\hat{z}\bullet\nabla a\times\nabla b=a_x b_y-a_y b_x$, and the inner product of the gradients: $(a,b)\equiv\nabla a\bullet\nabla b=a_x b_x+a_y b_y$, where subscripts here denote partial differentiation. Also, time derivatives have been denoted with a dot: i.e. $\dot{U}\equiv\partial U/\partial t$.

Next consider the field equations. Substitution into Equations (2.1a), (2.1d), and (2.2) yields:

$$\dot{n}+[n,U]+\left(n,\chi\right)+n\nabla^2\chi=0$$
(3.7)

$$\dot{p}_e + [p_e, U] + (p_e, \chi) + \gamma p_e \nabla^2 \chi = S_{pe} \tag{3.8}$$

$$\dot{p} + [p, U] + (p, \chi) + \gamma p \nabla^2 \chi = S_\kappa + S_P \tag{3.9}$$

The magnetic field evolution equation (2.1e), together with the Generalized Ohm's law (2.1f) yield, upon substitution:

$$\dot{\psi} + [\psi, U] + (\psi, \chi) = S_\psi \tag{3.10}$$

$$\dot{I} + [I, U] + (I, \chi) + I \nabla^2 \chi + [\psi, V_z] = S_I \tag{3.11}$$

Here, we have defined the effective source terms:

$$S_\kappa \equiv (\gamma - 1) \nabla \bullet [\kappa \nabla (p/n)]$$

$$S_p \equiv \frac{1}{n}[p_e, I] - \gamma \frac{p_e}{n^2}[n, I]$$

$$+ (\gamma - 1)\left[ \begin{array}{c} \eta \left( |\nabla^2 \psi|^2 + |\nabla I|^2 \right) \\ + \lambda \eta \left( |\nabla(\nabla^2 \psi)|^2 + I_{xx}^2 + I_{yy}^2 + 2I_{xy}^2 \right) \end{array} \right] \tag{3.12}$$

$$+ (\gamma - 1)\left[ \begin{array}{c} \mu \left[ (\chi_{xx} - \chi_{yy} + 2U_{xy})^2 + (U_{yy} - U_{xx} + 2\chi_{xy})^2 \right] \\ + (2\mu_C - \mu)|\nabla^2 \chi|^2 + \mu(V_z, V_z) \end{array} \right]$$

$$S_{pe} \equiv \frac{1}{n}[p_e, I] - \gamma \frac{p_e}{n^2}[n, I]$$

$$+ (\gamma - 1)\left[ \begin{array}{c} \nabla \bullet \kappa_e \nabla (p_e/n) + \eta \left( |\nabla^2 \psi|^2 + |\nabla I|^2 \right) \\ + \lambda \eta \left( |\nabla(\nabla^2 \psi)|^2 + I_{xx}^2 + I_{yy}^2 + 2I_{xy}^2 \right) + \alpha(p - 2p_e) \end{array} \right] \tag{3.13}$$

$$S_\psi \equiv \eta(\nabla^2 \psi - \lambda \nabla^4 \psi) + d_i n^{-1}[\psi, I] \tag{3.14}$$

$$S_I \equiv \eta(\nabla^2 I - \lambda \nabla^4 I) + d_i n^{-1}[\nabla^2 \psi, \psi] + d_i \nabla^2 \psi [n^{-1}, \psi] + d_i I[n^{-1}, I] + d_i[n^{-1}, p_e] \tag{3.15}$$

Note that we have neglected (assumed small) terms proportional to the gradients of $\eta, \mu, \mu_C$, and of $\lambda$, and have introduced the inverse equi-partition time: $\alpha \equiv 3m_e/(M_i \tau_e)$. The parameter $d_i$ that appears in the source terms (3.14) and (3.15) is equal to unity for the standard normalization given in Eq. (2.8), but is included so that we can easily change the ion skin depth without changing other problem parameters or dimensions. When present, the scale length is $l_0 \equiv c/(d_i \omega_{pi})$.

## IV. The Implicit Time Advance Equations for the Velocity Variables

The ideal MHD wave characteristics are contained in both the velocity advance and the field advance equations. In order to combine these into a single, higher order equation for efficient implicit solution, we next introduce the implicitness parameter $0<\theta<1$ and use this to evaluate the velocity variables in the field evolution Equations (3.7) and (3.9)-(3.11) at an advanced time for substitution into the momentum equations. Thus, Taylor expanding the velocity variables in these equations about the present time $t^n$ to evaluate at time $t^n+\theta\delta t$ yields:

$$\dot{n} + [n, U + \theta\delta t\dot{U}] + (n, \chi + \theta\delta t\dot{\chi}) + n\nabla^2(\chi + \theta\delta t\dot{\chi}) = 0 \tag{4.1}$$

$$\dot{p} + [p, U + \theta\delta t\dot{U}] + (p, \chi + \theta\delta t\dot{\chi}) + \gamma p\nabla^2(\chi + \theta\delta t\dot{\chi}) = S_\kappa + S_p \tag{4.2}$$

$$\dot{\psi} + [\psi, U + \theta\delta t\dot{U}] + (\psi, \chi + \theta\delta t\dot{\chi}) = S_\psi \tag{4.3}$$

$$\dot{I} + [I, U + \theta\delta t\dot{U}] + (I, \chi + \theta\delta t\dot{\chi}) + I(\nabla^2\chi + \theta\delta t\nabla^2\dot{\chi}) + [\psi, V_z + \theta\delta t\dot{V}_z] = S_I \tag{4.4}$$

Consider now the integrand for the weak form of the first momentum equation, (3.4). Similarly Taylor expanding the velocity and field variables in time, again using the implicitness parameter $\theta$, and substituting in from the field equations (4.1)-(4.4) for the time derivatives of the field variables that appear gives the implicit form of the first velocity equation:

$$
\begin{aligned}
&-n(v_i, \dot{U}) + n[v_i, \dot{\chi}] - n\nabla^2 U[v_i, U] + \tfrac{1}{2}n[v_i, (U,U)] - n\nabla^2 U(v_i, \chi) + [n, v_i][\chi, U] \\
&\quad + \tfrac{1}{2}n[v_i, (\chi, \chi)] + \nabla^2\psi[v_i, \psi] - gv_i n_x - \mu\nabla^2 v_i\nabla^2 U \\
&+\theta\delta t \left\{ \begin{array}{l} -n\nabla^2\dot{U}[v_i, U] - n\nabla^2 U[v_i, \dot{U}] + n[v_i, (U, \dot{U})] + n[v_i, (\chi, \dot{\chi})] - n\nabla^2\dot{U}(v_i, \chi) \\ -n\nabla^2 U(v_i, \dot{\chi}) + [n, v_i][\dot{\chi}, U] + [n, v_i][\chi, \dot{U}] - \mu\nabla^2 v_i\nabla^2\dot{U} \end{array} \right\} \\
&+\theta\delta t \left\{ \begin{array}{l} ([\psi, U], [v_i, \psi]) + ((\psi, \chi), [v_i, \psi]) - \nabla^2\psi[v_i, [\psi, U]] - \nabla^2\psi[v_i, (\psi, \chi)] \\ + gv_{ix}[n, U] + gv_{ix}(n, \chi) + gv_{ix}n\nabla^2\chi - (S_\psi, [v_i, \psi]) + \nabla^2\psi[v_i, S_\psi] \end{array} \right\} \\
&+(\theta\delta t)^2 \left\{ \begin{array}{l} ([\psi, \dot{U}], [v_i, \psi]) + ((\psi, \dot{\chi}), [v_i, \psi]) - \nabla^2\psi[v_i, [\psi, \dot{U}]] - \nabla^2\psi[v_i, (\psi, \dot{\chi})] \\ + gv_{ix}[n, \dot{U}] + gv_{ix}(n, \dot{\chi}) + gv_{ix}n\nabla^2\dot{\chi} \end{array} \right\} = 0
\end{aligned}
\tag{4.5}
$$

Note that since the purpose of this was to isolate and make implicit the wave motion, the density needed to be expanded only when it multiplied the gravitational term. We observe that the time derivatives of two of the velocity variables, $\dot{U}$ and $\dot{\chi}$, appear in many places at this stage. Next, expanding all the scalar variables as in equation (3.2) and integrating over the domain, we make use of the definitions in Appendix A to rewrite equation (4.5) as the system of discrete equations:

$$G_{i,j,k}^2 N_k \dot{U}_j + K_{i,j,k} N_k \dot{X}_j + V_{i,j,k,l}^1 N_l U_k U_j + V_{i,j,k,l}^3 N_l X_k U_j + V_{i,j,k,l}^5 N_l X_k X_j - G_{i,j,k} \Psi_j \Psi_k$$

$$+gX_{i,j}^0 N_j + \mu G_{i,j,k}^3 U_j N_k + \theta\delta t \left\{ \begin{array}{l} V_{i,j,k,l}^1 N_l [\dot{U}_k U_j + U_k \dot{U}_j] + V_{i,j,k,l}^3 N_l [\dot{X}_k U_j + \dot{X}_k \dot{U}_j] \\ +V_{i,j,k,l}^5 N_l [\dot{X}_k X_j + X_k \dot{X}_j] + \mu G_{i,j,k}^3 \dot{U}_j N_k \end{array} \right\}$$

$$+\theta\delta t \left\{ \begin{array}{l} C_{i,j,k,l}^1 \Psi_k \Psi_l U_j + C_{i,j,k,l}^3 \Psi_k \Psi_l X_j - [G_{i,j,k} + G_{i,k,j}] S_{\psi k} \Psi_j \\ +g[X_{i,j,k}^1 N_k U_j + X_{i,j,k}^2 N_k X_j] \end{array} \right\} \tag{4.6}$$

$$+(\theta\delta t)^2 \left\{ C_{i,j,k,l}^1 \Psi_k \Psi_l \dot{U}_j + C_{i,j,k,l}^3 \Psi_k \Psi_l \dot{X}_j + g[X_{i,j,k}^1 N_k \dot{U}_j + X_{i,j,k}^2 N_k \dot{X}_j] \right\} = 0$$

Summation over repeated indices is implied. We next multiply by the time step, $\delta t$, and center the time derivatives about time $t = (n+1/2)\delta t$, so that $\delta t \dot{U}_j = \left[ U_j^{n+1} - U_j^n \right]$, etc. . Express all state variables as the sum of an equilibrium part and a perturbed part; i.e. $U_j^n \to U_j^n + U_j^0$, etc. We can then put equation (4.6) in the form

$$S_{11}^v U^{n+1} + S_{12}^v V_z^{n+1} + S_{13}^v X^{n+1} = D_{11}^v U^n + D_{12}^v V_z^n + D_{13}^v X^n + R_{11}^v \Psi^n + R_{12}^v I^n + R_{13}^v P^n + O_1^v \tag{4.7}$$

Here, the block matrix elements are defined as:

$$S_{11}^v U^{n+1} = \left\{ \begin{array}{l} N_k G_{i,j,k}^2 + \theta\delta t\left[ -\mu B_{i,j} + N_l\left( V_{i,j,k,l}^1 + V_{i,j,k,l}^2 \right)\left( U_k + U_k^0 \right) + N_l V_{i,j,k,l}^3 (X_k + X_k^0) \right] \\ +\theta^2\delta t^2\left[ C_{i,j,k,l}^1 (\Psi_l + \Psi_l^0)(\Psi_k + \Psi_k^0) + gX_{i,j,k}^1 N_k \right] \end{array} \right\} U_j^{n+1}$$

$$S_{12}^v V_z^{n+1} = 0$$

$$S_{13}^v X^{n+1} = \left\{ \begin{array}{l} N_k K_{i,j,k} + \theta\delta t N_l[(U_k + U_k^0)V_{i,j,k,l}^4 + \left( V_{i,j,k,l}^5 + V_{i,j,k,l}^6 \right)(X_k + X_k^0)] \\ +\theta^2\delta t^2\left[ C_{i,j,k,l}^3 (\Psi_l + \Psi_l^0)(\Psi_k + \Psi_k^0) + gX_{i,j,k}^2 N_k \right] \end{array} \right\} X_j^{n+1}$$

$$D_{11}^v U^n = \left\{ \begin{array}{l} N_k G_{i,j,k}^2 + \delta t \left( \begin{array}{l} (1-\theta)\mu B_{i,j} + (V_{i,j,k,l}^1 + V_{i,j,k,l}^2)N_l\left[ \theta(U_k + U_k^0) - (\tfrac{1}{2}U_k + U_k^0) \right] \\ +V_{i,j,k,l}^3 N_l\left[ \theta(X_k + X_k^0) - (\tfrac{1}{2}X_k + X_k^0) \right] \end{array} \right) \\ +\theta(\theta-1)\delta t^2\left[ C_{i,j,k,l}^1 (\Psi_l + \Psi_l^0)(\Psi_k + \Psi_k^0) + gX_{i,j,k}^1 N_k \right] \end{array} \right\} U_j^n$$

$$D_{12}^v V_z^n = 0$$

$$D_{13}^v X^n = \left\{ \begin{array}{l} N_k K_{i,j,k} + \delta t N_l \left( \begin{array}{l} V_{i,j,k,l}^4\left[ \theta(U_k + U_k^0) - (\tfrac{1}{2}U_k + U_k^0) \right] \\ \left( V_{i,j,k,l}^5 + V_{i,j,k,l}^6 \right)\left[ \theta(X_k + X_k^0) - (\tfrac{1}{2}X_k + X_k^0) \right] \end{array} \right) \\ +\theta(\theta-1)\delta t^2\left[ C_{i,j,k,l}^3 (\Psi_l + \Psi_l^0)(\Psi_k + \Psi_k^0) + gX_{i,j,k}^2 N_k \right] \end{array} \right\} X_j^n$$

$$R_{11}^v \Psi^n = \begin{cases} \delta t(\tfrac{1}{2}\Psi_k + \Psi_k^0)(G_{i,j,k} + G_{i,k,j}) + \theta\delta t^2(G_{i,j,k} + G_{i,k,j})(S_{\psi k}^0 + S_{\psi k}) \\ \quad - \theta\delta t^2\left[\left(C_{i,k,l,j}^3 + C_{i,k,j,l}^3\right)X_k^0 + \left(C_{i,k,j,l}^1 + C_{i,k,l,j}^1\right)U_k^0\right]\left(\tfrac{1}{2}\Psi_l + \Psi_l^0\right) \end{cases} \Psi_j^n$$

$$R_{12}^v I^n = 0$$

$$R_{13}^v P^n = 0$$

$$O_1^v = \theta\delta t^2(G_{i,j,k} + G_{i,k,j})S_{\psi k}\Psi_j^0 + \delta t g X_{i,j}^0 N_j$$

A similar procedure is applied to the second and third momentum equation. We make use of the definitions in Appendix A to define the additional block matrix elements:

$$S_{21}^v U^{n+1} = \left\{\theta\delta t N_l V_{i,j,k,l}^8(V_{zk}^n + V_{zk}^0) - (\theta\delta t)^2 C_{i,j,k,l}^5(\Psi_k + \Psi_k^0)(I_l + I_l^0)\right\}U_j^{n+1}$$

$$S_{22}^v V_z^{n+1} = \begin{cases} N_k K_{i,j,k}^1 + \theta\delta t\left[-\mu\left(A_{i,j} - hB_{i,j}\right) + N_l V_{i,j,k,l}^7(U_k + U_k^0) + V_{i,j,k,l}^9 N_l(X_k + X_k^0)\right] \\ -\theta^2\delta t^2 C_{i,j,k,l}^9(\Psi_k + \Psi_k^0)(\Psi_l + \Psi_l^0) \end{cases} V_{zj}^{n+1}$$

$$S_{23}^v X^{n+1} = \left\{\theta\delta t N_l V_{i,j,k,l}^{10}(V_{zk}^n + V_{zk}^0) - (\theta\delta t)^2 C_{i,j,k,l}^7(\Psi_k + \Psi_k^0)(I_l + I_l^0)\right\}X_j^{n+1}$$

$$D_{21}^v U^n = \left\{\delta t V_{i,j,k,l}^8 N_l\left[\theta(V_{zk}^n + V_{zk}^0) - (\tfrac{1}{2}V_{zk}^n + V_{zk}^0)\right] - \theta(\theta-1)\delta t^2 C_{i,j,k,l}^5(\Psi_l + \Psi_l^0)(I_l + I_l^0)\right\}U_j^n$$

$$D_{22}^v V_z^n = \begin{cases} K_{i,j,k}^1 N_k + \delta t\begin{pmatrix}(1-\theta)\mu\left(A_{i,j} - hB_{i,j}\right) + N_l V_{i,j,k,l}^7\left[\theta(U_k + U_k^0) - (\tfrac{1}{2}U_k + U_k^0)\right] \\ + N_l V_{i,j,k,l}^9\left[\theta(X_k + X_k^0) - (\tfrac{1}{2}X_k + X_k^0)\right]\end{pmatrix} \\ -\theta(\theta-1)\delta t^2 C_{i,j,k,l}^9(\Psi_k + \Psi_k^0)(\Psi_l + \Psi_l^0) \end{cases} V_{zj}^n$$

$$D_{23}^v X^n = \left\{\delta t V_{i,j,k,l}^{10} N_l\left[\theta(V_{zk}^n + V_{zk}^0) - (\tfrac{1}{2}V_{zk}^n + V_{zk}^0)\right] - \theta(\theta-1)\delta t^2 C_{i,j,k,l}^7(\Psi_k + \Psi_k^0)(I_l + I_l^0)\right\}X_j^n$$

$$R_{21}^v \psi^n = \begin{cases} -\delta t K_{i,j,k}(\tfrac{1}{2}I_k + I_k^0) + \theta\delta t^2\begin{bmatrix}-K_{i,j,k}S_{lk} + \left(C_{i,k,j,l}^5 U_k^0 + C_{i,k,j,l}^7 X_k^0\right)(\tfrac{1}{2}I_l + I_l^0) \\ + \left(C_{i,k,j,l}^9 + C_{i,k,l,j}^9\right)(\tfrac{1}{2}\Psi_l + \Psi_l^0)V_k^0\end{bmatrix} \end{cases} \Psi_j$$

$$R_{22}^v I^n = \left\{-\delta t K_{i,k,j}(\tfrac{1}{2}\Psi_k + \Psi_k^0) + \theta\delta t^2\left[\left(C_{i,l,k,j}^5 U_l^0 + C_{i,l,k,j}^7 X_l^0\right)(\tfrac{1}{2}\Psi_k + \Psi_k^0)\right] - K_{i,k,j}(S_{\psi k}^0 + S_{\psi k})\right\}I_j$$

$$R_{23}^v P^n = 0$$

$$O_2^v = -\theta\delta t^2\left(K_{i,j,k}S_{lk}\Psi_j^0 + K_{i,k,j}S_{\psi k}I_j^0\right)$$

$$S_{31}^v U^{n+1} = \left\{ \begin{array}{l} -K_{i,j,k}N_k + \theta\delta t N_l\left[ V_{i,j,k,l}^{12}(X_k + X_k^0) + (V_{i,j,k,l}^{16} + V_{i,j,k,l}^{15})(U_k + U_k^0) \right] \\ +(\theta\delta t)^2 \left[ \begin{array}{l} C_{i,j,k,l}^{11}(\Psi_k + \Psi_k^0)(\Psi_l + \Psi_l^0) + C_{i,j,k,l}^{15}(I_k + I_k^0)(I_l + I_l^0) \\ -G_{i,j,k}^7(P_k + P_k^0) - gY_{i,j,k}^1 N_k \end{array} \right] \end{array} \right\} U_j^{n+1}$$

$$S_{32}^v V_z^{n+1} = (\theta\delta t)^2 C_{i,j,k,l}^{15}(\Psi_k + \Psi_k^0)(I_l + I_l^0)V_j^{n+1}$$

$$S_{33}^v X^{n+1} = \left\{ \begin{array}{l} G_{i,j,k}^2 N_k + \theta\delta t\left[ -2\mu_C B_{i,j} + N_l V_{i,j,k,l}^{11}(U_k + U_k^0) + N_l(V_{i,j,k,l}^{13} + V_{i,j,k,l}^{14})(X_k + X_k^0) \right] \\ +(\theta\delta t)^2 \left[ \begin{array}{l} C_{i,j,k,l}^{13}(\Psi_k + \Psi_k^0)(\Psi_l + \Psi_l^0) + C_{i,j,k,l}^{17}(I_k + I_k^0)(I_l + I_l^0) \\ -(G_{i,j,k}^{6A} + \gamma G_{i,j,k}^{6B})(P_k + P_k^0) - gY_{i,j,k}^2 N_k + C_{i,j,k,l}^{17} I_l^{0SI} I_k^{0SI} \end{array} \right] \end{array} \right\} X_j^{n+1}$$

$$D_{31}^v U^n = \left\{ \begin{array}{l} -K_{i,j,k}N_k + \delta t N_l\left[ \begin{array}{l} V_{i,j,k,l}^{12}[\theta(X_k + X_k^0) - (\tfrac{1}{2}X_k + X_k^0)] \\ +(V_{i,j,k,l}^{15} + V_{i,j,k,l}^{16})[\theta(U_k + U_k^0) - (\tfrac{1}{2}U_k + U_k^0)] \end{array} \right] \\ +\theta(\theta - 1)\delta t^2 \left[ \begin{array}{l} C_{i,j,k,l}^{11}(\Psi_k + \Psi_k^0)(\Psi_l + \Psi_l^0) + C_{i,j,k,l}^{15}(I_k + I_k^0)(I_l + I_l^0) \\ -G_{i,j,k}^7(P_k + P_k^0) - gY_{i,j,k}^1 N_k \end{array} \right] \end{array} \right\} U_j^n$$

$$D_{32}^v V_z^n = \theta(\theta - 1)\delta t^2 C_{i,j,k,l}^{15}(\Psi_k + \Psi_k^0)(I_l + I_l^0)V_j^n$$

$$D_{33}^v X^n = \left\{ \begin{array}{l} G_{i,j,k}^2 N_k + \delta t \left[ \begin{array}{l} (1-\theta)2\mu_C B_{i,j} + N_l V_{i,j,k,l}^{11}[\theta(U_k + U_k^0) - (\tfrac{1}{2}U_k + U_k^0)] \\ +N_l(V_{i,j,k,l}^{13} + V_{i,j,k,l}^{14})[\theta(X_k + X_k^0) - (\tfrac{1}{2}X_k + X_k^0)] \end{array} \right] \\ \quad + \theta(\theta - 1)\delta t^2 \left[ \begin{array}{l} C_{i,j,k,l}^{13}(\Psi_k + \Psi_k^0)(\Psi_l + \Psi_l^0) + C_{i,j,k,l}^{17}(I_k + I_k^0)(I_l + I_l^0) \\ -(G_{i,j,k}^{6A} + \gamma G_{i,j,k}^{6B})(P_k + P_k^0) - gY_{i,j,k}^2 N_k \end{array} \right] \\ +(\theta\delta t)^2 C_{i,j,k,l}^{17} I_k^{0SI} I_l^{0SI} \end{array} \right\} X_j^n$$

$$R_{31}^v \Psi^n = \left\{ \begin{array}{l} \delta t\left[ G_{i,k,j}^4 + G_{i,j,k}^4 \right](\tfrac{1}{2}\Psi_k + \Psi_k^0) \\ -\theta\delta t^2 \left[ \begin{array}{l} \left([C_{i,k,j,l}^{11} + C_{i,k,l,j}^{11}]U_k^0 + [C_{i,k,j,l}^{13} + C_{i,k,l,j}^{13}]X_k^0\right)(\tfrac{1}{2}\Psi_l + \Psi_l^0) \\ +C_{i,k,j,l}^{19}V_k^0(\tfrac{1}{2}I_l + I_l^0) + H_{i,j,k}^3(S_{\psi k}^0 + S_{\psi k}) \end{array} \right] \end{array} \right\} \Psi_j$$

$$R_{32}^v I^n = \left\{ \begin{array}{l} \delta t\left[ G_{i,k,j}^5 + G_{i,j,k}^5 \right](\tfrac{1}{2}I_k + I_k^0) \\ -\theta\delta t^2 \left[ \begin{array}{l} \left([C_{i,k,j,l}^{15} + C_{i,k,l,j}^{15}]U_k^0 + [C_{i,k,j,l}^{17} + C_{i,k,l,j}^{17}]X_k^0\right)(\tfrac{1}{2}I_l + I_l^0) \\ +C_{i,l,k,j}^{19}V_l^0(\tfrac{1}{2}\Psi_k + \Psi_k^0) + H_{i,j,k}^5(S_{Ik}^0 + S_{Ik}) \end{array} \right] \end{array} \right\} I_j$$

$$R_{33}^v P^n = \left\{ -\delta t A_{i,j} + \theta\delta t^2\left[ G_{i,k,j}^7 U_k^0 + G_{i,k,j}^6 X_k^0 \right] \right\} P_j$$

$$O_v^3 = -\theta\delta t^2 \left\{ H_{i,j,k}^3 S_{\psi k}\Psi_j^0 + H_{i,j,k}^5 S_{Ik} I_j^0 + A_{i,j}\left( S_{pj} + S_{\kappa j} \right) \right\} - \delta t g Y_{i,j}^0 N_j$$

Here, we have defined the auxiliary source variables satisfying the following matrix equations. (Note that equilibrium and perturbed pieces are defined separately in the normal way.)

$$D_{i,j}(S_{\psi j} + S_{\psi j}^0) = \eta\left(A_{i,j} - \lambda B_{i,j}\right)(\Psi_j + \Psi_j^0) + V_{i,j,k,l}^7 E_l(\Psi_j + \Psi_j^0)(I_k + I_k^0)$$

$$D_{i,j}(S_{Ij} + S_{Ij}^0) = \eta\left(A_{i,j} - \lambda B_{i,j}\right)(I_j + I_j^0) + U_{i,j,k,l}^1 E_l(\Psi_j + \Psi_j^0)(\Psi_k + \Psi_k^0)$$

$$+ U_{i,j,k,l}^3 E_j(I_k + I_k^0)(I_l + I_l^0) + K_{i,j,k}^0 E_j(P_{ek} + P_{ek}^0)$$

$$D_{i,j}S_{\kappa j} = (\gamma - 1)\kappa_T\left[G_{i,k,j}^2 + G_{i,j,k}^2 - h_p G_{i,k,j}^{13}\right]E_k\left(P_j + P_j^0\right)$$

$$D_{i,j}S_{pj} = U_{i,j,k,l}^5 N_l\left(P_{ej} + P_{ej}^0\right)\left(I_k + I_k^0\right)$$

$$+ (\gamma - 1)\left\{\begin{array}{l} \mu\left[G_{i,j,k}^{14}U_jU_k + G_{i,j,k}^{15}\chi_j\chi_k + G_{i,j,k}^{16}U_j\chi_k - G_{k,j,i}^2 V_{zj}V_{zk}\right] \\ + 2(\mu_C - \mu)G_{i,j,k}^{17}\chi_j\chi_k + \eta\left(K_{i,j,k}^1 - \lambda G_{k,j,i}^2\right)\left(J_k + J_k^0\right)\left(J_j + J_j^0\right) \\ + \eta\left(-G_{k,j,i}^2 + \lambda G_{i,j,k}^{12}\right)\left(I_k + I_k^0\right)\left(I_j + I_j^0\right) \end{array}\right\}$$

We have also introduced a variable for the reciprocal of the density: $\quad 1/n = \sum_{j=1}^{18} v_j E_j$.

With these definitions, the 3 momentum equations are combined into the single block matrix equation:

$$\begin{bmatrix} S_{11}^v & S_{12}^v & S_{13}^v \\ S_{21}^v & S_{22}^v & S_{23}^v \\ S_{31}^v & S_{32}^v & S_{33}^v \end{bmatrix} \bullet \begin{bmatrix} U \\ V_z \\ X \end{bmatrix}^{n+1} = \begin{bmatrix} D_{11}^v & D_{12}^v & D_{13}^v \\ D_{21}^v & D_{22}^v & D_{23}^v \\ D_{31}^v & D_{32}^v & D_{33}^v \end{bmatrix} \bullet \begin{bmatrix} U \\ V_z \\ X \end{bmatrix}^n + \begin{bmatrix} R_{11}^v & R_{12}^v & R_{13}^v \\ R_{21}^v & R_{22}^v & R_{23}^v \\ R_{31}^v & R_{32}^v & R_{33}^v \end{bmatrix}\begin{bmatrix} \psi \\ I \\ P \end{bmatrix}^n + \begin{bmatrix} O_1^v \\ O_2^v \\ O_3^v \end{bmatrix} \quad (4.15)$$

This compact equation contains within it all of the MHD wave characteristics. By factoring the matrix on the left and solving this system, we are able to take time steps that are not limited by the Courant condition based on the MHD waves in the system or by any diffusive phenomena. We note here that equation (4.15) has two important sub-systems that can be solved in a fraction of the run time of the full system. Keeping only the terms in the upper left corners in the three matrices gives the 2-field reduced MHD system considered in [3]. Keeping only the upper left 2 × 2 sub-blocks gives the 4-field system discussed in [4]. These reduced systems are valuable for both debugging the full system, and for better understanding the incremental physical effects that the full system introduces.


## V. The Implicit Field Equations:
Once the velocity variables are updated to the new time, the density equation can be updated independent of the other field equations. Again, using the implicitness parameter $\theta$ to evaluate quantities at the advanced time, we define the matrix elements:

$$S_{11}^n N_j^{n+1} = \left\{ D_{i,j} + \theta \delta t \left[ K_{i,j,k}(U_k + U_k^0) + G_{i,k,j}^2 (X_k + X_k^0) \right] \right\} N_j^{n+1}$$

$$D_{11}^n N_j^n = \left\{ \begin{array}{l} D_{i,j} + \delta t K_{i,j,k}[\theta(U_k + U_k^0) - (\tfrac{1}{2} U_k^n + U_k^0)] \\ + \delta t G_{i,k,j}^2[\theta(X_k + X_k^0) - (\tfrac{1}{2} X_k^n + X_k^0)] \end{array} \right\} N_j^n$$

$$R_{11}^n U_j^{n+1} = -\theta \delta t K_{i,k,j}(N_k + N_k^0) U_j^{n+1}$$

$$R_{12}^n = 0$$

$$R_{13}^n X_j^{n+1} = -\theta \delta t G_{i,j,k}^2 (N_k + N_k^0) X_j^{n+1}$$

$$Q_{11}^n U_j^n = -\delta t K_{i,k,j}[(\tfrac{1}{2} N_k^n + N_k^0) - \theta(N_k + N_k^0)] U_j^n$$

$$Q_{12}^n = 0$$

$$Q_{13}^n X_j^n = -\delta t G_{i,j,k}^2[(\tfrac{1}{2} N_k + N_k^0) - \theta(N_k + N_k^0)] X_j^n$$

These allow us to write the implicit density advance as a block matrix equation:

$$S_{11}^n \bullet N^{n+1} = D_{11}^n \bullet N^n + \begin{bmatrix} R_{11}^n & R_{12}^n & R_{13}^n \end{bmatrix} \bullet \begin{bmatrix} U \\ V_z \\ X \end{bmatrix}^{n+1} + \begin{bmatrix} Q_{11}^n & Q_{12}^n & Q_{13}^n \end{bmatrix} \bullet \begin{bmatrix} U \\ V_z \\ X \end{bmatrix}^n \tag{5.1}$$

In a similar way, for the pressure advance we define the block matrix elements:

$$S_{11}^p P_j^{n+1} = \left\{ \begin{array}{l} D_{i,j} + \theta \delta t K_{i,j,k}(U_k + U_k^0) \\ -\theta \delta t (\gamma - 1)\kappa \left( G_{i,j,k} + G_{i,k,j} \right) E_k \\ + \theta \delta t [G_{i,k,j}^2 - (\gamma - 1) K_{i,k,j}^2](X_k + X_k^0) \end{array} \right\} P_j^{n+1}$$

$$D_{11}^p P_j^n = \left\{ \begin{array}{l} D_{i,j} + \delta t K_{i,j,k}[\theta(U_k + U_k^0) - (\tfrac{1}{2} U_k^n + U_k^0)] \\ + (1-\theta)\delta t (\gamma - 1)\kappa \left( G_{i,j,k} + G_{i,k,j} \right) E_k \\ + \delta t [G_{i,k,j}^2 - (\gamma - 1) K_{i,k,j}^2][\theta(X_k + X_k^0) - (\tfrac{1}{2} X_k^n + X_k^0)] \end{array} \right\} P_j^n$$

$$R_{11}^p U_j^{n+1} = -\theta \delta t K_{i,k,j}(P_k + P_k^0) U_j^{n+1}$$

$$R_{12}^p = 0$$

$$R_{13}^p X_j^{n+1} = -\theta \delta t [G_{i,j,k}^2 - (\gamma - 1) K_{i,j,k}^2](P_k + P_k^0) X_j^{n+1}$$

$$Q_{11}^p U_j^n = -\delta t K_{i,k,j}[(\tfrac{1}{2} P_k^n + P_k^0) - \theta(P_k + P_k^0)] U_j^n$$

$$Q_{12}^p = 0$$

$$Q_{13}^p X_j^n = -\delta t [G_{i,j,k}^2 - (\gamma - 1) K_{i,j,k}^2][(\tfrac{1}{2} P_k + P_k^0) - \theta(P_k + P_k^0)] X_j^n$$

$$O_1^p = \delta t \left[ D_{i,j} S_{pj} + (\gamma - 1)\kappa \left[ G_{i,k,j}^2 + G_{i,j,k}^2 - h_p G_{i,k,j}^{13} \right] E_k P_j^0 \right]$$

Using these, the pressure equation can be written as:

$$S_{11}^p \bullet P^{n+1} = D_{11}^p \bullet P^n + \begin{bmatrix} R_{11}^p & R_{12}^p & R_{13}^p \end{bmatrix} \bullet \begin{bmatrix} U \\ V_z \\ X \end{bmatrix}^{n+1} + \begin{bmatrix} Q_{11}^p & Q_{12}^p & Q_{13}^p \end{bmatrix} \bullet \begin{bmatrix} U \\ V_z \\ X \end{bmatrix}^n + O_1^p \qquad (5.2)$$

Next, consider the remaining field equations for the two components of the magnetic field and for the electron pressure. These are solved simultaneously in order to capture the coupling that leads to the Whistler and kinetic Alfven modifications to the MHD waves. Thus, in a similar manner, we form a set of implicit equations for the field and electron pressure variables by Taylor expanding all variables in time and keeping the terms linear in $\delta t$. Applying the Galerkin method and making use of the definitions in Appendix A yields the following block matrix form for these remaining time advance equations:

$$
\begin{bmatrix} S_{11}^b & S_{12}^b & S_{13}^b \\ S_{21}^b & S_{22}^b & S_{23}^b \\ S_{31}^b & S_{32}^b & S_{33}^b \end{bmatrix} \begin{bmatrix} \psi \\ I \\ P_e \end{bmatrix}^{n+1} = \begin{bmatrix} D_{11}^b & D_{12}^b & D_{13}^b \\ D_{21}^b & D_{22}^b & D_{23}^b \\ D_{31}^b & D_{32}^b & D_{33}^b \end{bmatrix} \bullet \begin{bmatrix} \psi \\ I \\ P_e \end{bmatrix}^n + \begin{bmatrix} R_{11}^b & R_{12}^b & R_{13}^b \\ R_{21}^b & R_{22}^b & R_{23}^b \\ R_{31}^b & R_{32}^b & R_{33}^b \end{bmatrix} \bullet \begin{bmatrix} U \\ V_z \\ X \end{bmatrix}^{n+1}
$$
$$
+ \begin{bmatrix} Q_{11}^b & Q_{12}^b & Q_{13}^b \\ Q_{21}^b & Q_{22}^b & Q_{23}^b \\ Q_{31}^b & Q_{32}^b & Q_{33}^b \end{bmatrix} \bullet \begin{bmatrix} U \\ V_z \\ X \end{bmatrix}^n + \begin{bmatrix} O_1 \\ O_2 \\ O_3 \end{bmatrix}
$$

$$\qquad (5.3)$$

The matrix elements are defined as follows:

$$S_{11}^b \Psi_j^{n+1} = \left\{ D_{i,j} + \theta \delta t \begin{bmatrix} K_{i,j,k}(U_k + U_k^0) - \eta(A_{i,j} - \lambda B_{i,j}) \\ -G_{j,k,i}^2(X_k + X_k^0) - d_i U_{i,j,k,l}^3 E_l(I_k + I_k^0) \end{bmatrix} \right\} \Psi_j^{n+1}$$

$$S_{12}^b I_j^{n+1} = -\theta \delta t d_i U_{i,j,k,l}^4 E_l(\Psi_k + \Psi_k^0) I_j^{n+1}$$

$$S_{13}^b = 0$$

$$D_{11}^b \Psi_j^n = \left\{ \begin{aligned} &D_{i,j} + \delta t K_{i,j,k}\left[\theta(U_k + U_k^0) - (\tfrac{1}{2}U_k + U_k^0)\right] + (\theta-1)\delta t \eta(A_{i,j} - \lambda B_{i,j}) \\ &- \delta t G_{j,k,i}^2\left[\theta(X_k + X_k^0) - (\tfrac{1}{2}X_k + X_k^0)\right] - \delta t d_i U_{i,j,k,l}^3 E_l\left[\theta(I_k + I_k^0) - (\tfrac{1}{2}I_k + I_k^0)\right] \end{aligned} \right\} \Psi_j^n$$

$$D_{12}^b I_j = -\left\{ \delta t d_i U_{i,j,k,l}^4 E_l\left[\theta(\Psi_k + \Psi_k^0) - (\tfrac{1}{2}\Psi_k + \Psi_k^0)\right] \right\} I_j$$

$$D_{13}^b = 0$$

$$R_{11}^b U_j^{n+1} = -\theta \delta t K_{i,k,j}(\Psi_k + \Psi_k^0) U_j^{n+1}$$

$$R_{12}^b = 0$$

$$R_{13}^b X_j^{n+1} = \theta \delta t G_{k,j,i}^2(\Psi_k + \Psi_k^0) X_j^{n+1}$$

$$O_1 = \delta t \eta\left(A_{i,j} - \lambda B_{i,j}\right) \Psi_j^0$$

14

$$Q_{11}^b U_j^n = \delta t K_{i,k,j} \left[ \theta(\Psi_k + \Psi_k^0) - (\tfrac{1}{2}\Psi_k + \Psi_k^0) \right] U_j^n$$

$$Q_{12}^b = 0$$

$$Q_{13}^b X_j^n = -\delta t G_{k,j,i}^2 \left[ \theta(\Psi_k + \Psi_k^0) - (\tfrac{1}{2}\Psi_k + \Psi_k^0) \right] X_j^n$$

$$S_{21}^b \Psi_j^{n+1} = \theta \delta t \left\{ K_{i,j,k}(V_{zk} + V_{zk}^0) - d_i(U_{i,j,k,l}^1 + U_{i,j,k,l}^2) E_l(\Psi_k + \Psi_k^0) \right\} \Psi_j^{n+1}$$

$$S_{22}^b I_j^{n+1} = \left[ D_{i,j} + \theta \delta t \begin{pmatrix} \eta(-A_{i,j} + \lambda B_{i,j}) + K_{i,j,k}(U_k + U_k^0) \\ + G_{i,k,j}^2(X_k + X_k^0) - d_i(U_{i,j,k,l}^5 + U_{i,j,k,l}^6)(I_k + I_k^0)E_l \end{pmatrix} \right] I_j^{n+1}$$

$$S_{23}^b P_{ej}^{n+1} = -\theta \delta t d_i K_{i,k,j} E_k P_{ej}^{n+1}$$

$$D_{21}^b \Psi_j^n = \delta t \left\{ K_{i,j,k} \left[ \theta(V_{zk} + V_{zk}^0) - (\tfrac{1}{2}V_{zk} + V_{zk}^0) \right] - d_i(U_{i,j,k,l}^1 + U_{i,j,k,l}^2)E_l \left[ \theta(\Psi_k + \Psi_k^0) - (\tfrac{1}{2}\Psi_k + \Psi_k^0) \right] \right\} \Psi_j^n$$

$$D_{22}^b I_j^n = \begin{cases} D_{i,j} + (\theta-1)\delta t \eta \left( -A_{i,j}\eta_k + \lambda B_{i,j} \right) + \delta t K_{i,j,k} \left[ \theta(U_k + U_k^0) - (\tfrac{1}{2}U_k + U_k^0) \right] \\ + \delta t G_{i,k,j}^2 \left[ \theta(X_k + X_k^0) - (\tfrac{1}{2}X_k + X_k^0) \right] - \delta t d_i(U_{i,j,k,l}^5 + U_{i,j,k,l}^6)E_l \left[ \theta(I_k + I_k^0) - (\tfrac{1}{2}I_k + I_k^0) \right] \end{cases} I_j^n$$

$$D_{23}^b P_{ej}^n = (1-\theta)\delta t d_i K_{i,k,j} E_k P_{ej}^n$$

$$R_{21}^b U_j^{n+1} = -\theta \delta t K_{i,k,j}(I_k + I_k^0) U_j^{n+1}$$

$$R_{22}^b V_{zj}^{n+1} = -\theta \delta t K_{i,k,j}(\Psi_k + \Psi_k^0) V_{zj}^{n+1}$$

$$R_{23}^b X_j^{n+1} = -\theta \delta t G_{i,j,k}^2(I_k + I_k^0) X_j^{n+1}$$

$$Q_{21}^b U_j^n = \delta t K_{i,k,j} \left[ \theta(I_k + I_k^0) - (\tfrac{1}{2}I_k + I_k^0) \right] U_j^n$$

$$Q_{22}^b V_{zj}^n = \delta t K_{i,k,j} \left[ \theta(\Psi_k + \Psi_k^0) - (\tfrac{1}{2}\Psi_k + \Psi_k^0) \right] V_{zj}^n$$

$$Q_{23}^b X_j^n = \delta t G_{i,j,k}^2 \left[ \theta(I_k + I_k^0) - (\tfrac{1}{2}I_k + I_k^0) \right] X_j^n$$

$$O_2 = \delta t \eta \left( A_{i,j} - \lambda B_{i,j} \right) I_j^0$$

$$S_{31}^b = 0$$

$$S_{32}^b I_j^{n+1} = -\theta \delta t d_i U_{i,j,k,l}^6(P_{ek} + P_{ek}^0) E_l I_j^{n+1}$$

$$S_{33}^b P_{ej}^{n+1} = \begin{cases} D_{i,j} \left[ 1 + 2\delta t \theta(\gamma-1)\alpha \right] + \theta \delta t K_{i,j,k}(U_k + U_k^0) \\ -\theta \delta t d_i U_{i,j,k,l}^6(P_{ek} + P_{ek}^0) E_l(V_{i,j,k,l}^7 + \gamma U_{i,j,k,l}^5) E_l(I_k + I_k^0) + \theta \delta t [G_{i,k,j}^2 - (\gamma-1)K_{i,k,j}^2](X_k + X_k^0) \\ -(\gamma-1)\theta \delta t \kappa \left\{ G_{i,k,j}^2 + G_{i,j,k}^2 - h_p G_{i,k,j}^{13} \right\} N_k \end{cases} P_{ej}^{n+1}$$

$$D_{31}^{b} = 0$$

$$D_{32}^{b} I_{j}^{n} = -\delta t d_{i} U_{i,j,k,l}^{6} E_{l} \left[ \theta(P_{ek} + P_{ek}^{0}) - (\tfrac{1}{2} P_{ek} + P_{ek}^{0}) \right] I_{j}^{n}$$

$$D_{33}^{b} P_{ej}^{n} = \left\{ \begin{array}{l} D_{i,j} \left[ 1 + 2\delta t(\theta-1)(\gamma-1)\alpha \right] + \delta t K_{i,j,k} \left[ \theta(U_{k} + U_{k}^{0}) - (\tfrac{1}{2} U_{k} + U_{k}^{0}) \right] \\[4pt] -\delta t d_{i} U_{i,j,k,l}^{6} (P_{ek} + P_{ek}^{0}) E_{l} (V_{i,j,k,l}^{7} + \gamma U_{i,j,k,l}^{5}) \left[ \theta(I_{k} + I_{k}^{0}) - (\tfrac{1}{2} I_{k} + I_{k}^{0}) \right] E_{l} \\[4pt] +\delta t [G_{i,k,j}^{2} - (\gamma-1) K_{i,k,j}^{2}] \left[ \theta(X_{k} + X_{k}^{0}) - (\tfrac{1}{2} X_{k} + X_{k}^{0}) \right] \\[4pt] +(\gamma-1)(1-\theta)\delta t \kappa \left\{ G_{k,j}^{2} + G_{j,k}^{2} - h_{p} G_{k,j}^{13} \right\} N_{k} \end{array} \right\} P_{ej}^{n}$$

$$R_{31}^{b} U_{j}^{n+1} = -\theta \delta t K_{i,k,j} (P_{ek} + P_{ek}^{0}) U_{j}^{n+1}$$

$$R_{32}^{b} = 0$$

$$R_{33}^{b} X_{j}^{n+1} = -\theta \delta t \left[ G_{i,j,k}^{2} - (\gamma-1) K_{i,j,k}^{2} \right] (P_{ek} + P_{ek}^{0}) X_{j}^{n+1}$$

$$Q_{31}^{b} U_{j}^{n} = \delta t K_{i,k,j} \left[ \theta(P_{ek} + P_{ek}^{0}) - (\tfrac{1}{2} P_{ek} + P_{ek}^{0}) \right] U_{j}^{n}$$

$$Q_{32}^{b} = 0$$

$$Q_{33}^{b} X_{j}^{n} = +\delta t \left[ G_{i,j,k}^{2} - (\gamma-1) K_{i,j,k}^{2} \right] \left[ \theta(P_{ek} + P_{ek}^{0}) - (\tfrac{1}{2} P_{ek} + P_{ek}^{0}) \right] X_{j}^{n}$$

$$O_{3} = \delta t(\gamma-1)\kappa \left\{ G_{i,k,j}^{2} + G_{i,j,k}^{2} - h_{p} G_{i,k,j}^{13} \right\} E_{k} P_{j}^{0} + \delta t (V_{i,j,k,l}^{7} + \gamma U_{i,j,k,l}^{5}) E_{l} I_{k}^{0} P_{ej}^{0}$$
$$+ \delta t(\gamma-1)\eta \left\{ \left( K_{i,j,k}^{1} - \lambda G_{k,j,i}^{2} \right) \left( J_{k} + J_{k}^{0} \right) \left( J_{j} + J_{j}^{0} \right) + \left( -G_{k,j,i}^{2} + \lambda G_{i,j,k}^{12} \right) \left( I_{k} + I_{k}^{0} \right) \left( I_{j} + I_{j}^{0} \right) \right\}$$
$$+ \delta t(\gamma-1)\alpha D_{i,j} P_{j}$$

## VI. Smoothing of velocity fields, a semi-implicit operator, and well posedness:

Here we describe three modifications to the previously described algorithm that serve to increase the robustness and nonlinear stability of the overall scheme.

The first is that we find it useful to incorporate a small "hyper-viscosity" term in the two momentum equations (3.4) and (3.6) in order to damp sub-element scale oscillations that might otherwise develop. Since these terms would involve 6th order derivatives of the $U$ and $\chi$ fields, they cannot be straightforwardly incorporated into the time advance using elements with only $C^{1}$ continuity unless we introduce additional variables. We therefore introduce a time splitting where the scalar functions $U$ and $\chi$ are first advanced without these terms, and then a "smoothing" step is applied where these operators are applied. Consider the split time advance for the vorticity. Let the time advance values at time level (n+1) but without these higher derivative operators applied be denoted by (*). The advance from level (*) to the new level (n+1) is given by:

$$w^* = \nabla^2 U^*$$
$$\nabla^2 U^{n+1} = w^* - \delta t \nu_H \left[ \theta \nabla^4 w^{n+1} + (1-\theta) \nabla^4 w^* \right]$$
$$w^{n+1} = \nabla^2 U^{n+1}$$
(6.1)

Multiply through by each trial function $\nu_i$, and this is equivalent to the two equations:

$$D_{i,j} W_j^* = A_{i,j} U_j^*$$
(6.2a)

and

$$\begin{bmatrix} D_{i,j} & -A_{i,j} \\ \delta t \nu_H \theta B_{i,j} & A_{i,j} \end{bmatrix} \begin{bmatrix} W \\ U \end{bmatrix}_j^{n+1} = \begin{bmatrix} 0 \\ \left[ D_{i,j} - \delta t \nu_H (1-\theta) B_{i,j} \right] W_j^* \end{bmatrix}$$
(6.2b)

Since these matrices on the left do not change during the simulation (if the timestep and element geometry are constant), they can be factored at the initial time and the equations are then solved each timestep by an efficient back-substitution. In the examples in this paper, a hyper-viscosity was used with the value $\nu_H = h^2 \mu$, where $h$ is a typical triangle dimension and $\mu$ is the viscosity. Rerunning several cases with half this value had essentially no noticeable effect on the computed results.

A second modification is that it is sometimes useful to add a semi-implicit term to help stabilize the $X$ equation. This is particularly true if the total magnetic field vanishes somewhere or is small at a point. To this end, we introduce an artificial "semi-implicit" magnetic field $I_k^{0SI}$ and modify the matrix elements as follows:

$$S_{33}^v \rightarrow S_{33}^v + (\theta \delta t)^2 C_{i,j,k,l}^{17} (I_k^{0SI})(I_l^{0SI})$$
$$D_{33}^v \rightarrow D_{33}^v + (\theta \delta t)^2 C_{i,j,k,l}^{17} (I_k^{0SI})(I_l^{0SI})$$
(6.3)

This modification was not used in the examples presented in this paper.

A third technique has to do with the solubility condition on equation (3.6). Before being multiplied by the trial function and integrated by parts, this equation for the time derivative of the divergence of the velocity had the form:

$$\nabla \cdot n \nabla \dot{\chi} = r \quad \text{in the interior}$$
$$\frac{\partial \dot{\chi}}{\partial n} = 0 \quad \text{on the boundary}$$
(6.4)

It is well known that equations of this type have a solubility constraint that may not be exactly satisfied numerically, and are indeterminate in that if $\chi$ is a solution, then $\chi + c$ is also a solution for any constant $c$. To address both of these, we shift the spectrum by replacing the first of the equations in (6.4) with:

$$(\nabla \cdot n \nabla - \varepsilon) \dot{\chi} = r$$
(6.5)

where $\varepsilon$ is some small number typically $10^{-7}$[15]. This is equivalent to adding a small positive definite term proportional to $\varepsilon\chi^2$ to the variational statement of equation (6.4) which will automatically seek the solution that minimizes $\varepsilon\chi^2$ as well as satisfies the differential equation.

## VII. Summary of the time advance:

Here we summarize and discuss the time advance equations given in Section VI. By defining the appropriate vector and matrix quantities, we can rewrite Eqns. (4.15), (5.1), (5.2), and (5.3) in the compact form:

$$\mathbf{S}^V \cdot \mathbf{V}^{n+1} = \mathbf{D}^V \cdot \mathbf{V}^n + \mathbf{R}^V \cdot \mathbf{\Psi}^n + \mathbf{O}^V \tag{7.1}$$

$$\mathbf{S}^N \cdot \mathbf{N}^{n+1} = \mathbf{D}^N \cdot \mathbf{N}^n + \left[\mathbf{R}^N\right]^\dagger \cdot \mathbf{V}^{n+1} + \left[\mathbf{Q}^N\right]^\dagger \cdot \mathbf{V}^n + \mathbf{O}^N \tag{7.2}$$

$$\mathbf{S}^P \cdot \mathbf{P}^{n+1} = \mathbf{D}^P \cdot \mathbf{P}^n + \left[\mathbf{R}^P\right]^\dagger \cdot \mathbf{V}^{n+1} + \left[\mathbf{Q}^P\right]^\dagger \cdot \mathbf{V}^n + \mathbf{O}^P \tag{7.3}$$

$$\mathbf{S}^B \cdot \mathbf{\Psi}^{n+1} = \mathbf{D}^B \cdot \mathbf{\Psi}^n + \mathbf{R}^B \cdot \mathbf{V}^{n+1} + \mathbf{Q}^B \cdot \mathbf{V}^n + \mathbf{O}^B \tag{7.4}$$

The matrices all contain the unknowns only at the old time level. The main computational work is in solving these matrix equations. If we have a grid system with M node points, then the matrices $\mathbf{S}^V$ and $\mathbf{S}^B$ are both sparse matrices of rank 18M, and the matrices $\mathbf{S}^N$ and $\mathbf{S}^P$ are sparse matrices of rank 6M. We use the parallel direct sparse solver, SuperLU_dist [19], and so the most computationally intensive part of the time advance is to factor these matrices. We note that the four matrices could be factored concurrently as there are no dependences (although this was not done in our examples). A typical run in Section X of 400 time-steps for the full 8-field system on a $121 \times 121$ grid point mesh required 13.2 hours using 2 nodes (each with 8 processors) on the NERSC IBM p575 Power 5 system (Bassi). We note that the timing is independent of the size of the time step since there are no iterations involved.

A model system that was amenable to stability analysis, but which has the essential features of (7.1) and (7.4), was shown to lead to an unconditionally stable numerical method for implicitness parameter $\theta > 1/2$ in [4]. We postulate that the full system presented here is also unconditionally stable for $\theta > 1/2$, and have observed this over a wide region in parameter space where we have used time steps $\delta t$ many times the Courant condition based on any of the waves, and, of course, many times the explicit time step restriction associated with the diffusive terms. We choose the time step based on accuracy considerations alone.

What constitutes consistent and stable boundary conditions for a computational study of an extended MHD plasma is still a subject of research. To circumvent this difficulty, we introduce a transition region where the ion skin depth parameter $d_i$ gets multiplied by a factor $f$ that is unity in the interior and vanishes at the wall. Thus, if the computational domain extends from $0 < x < L_x$ and $0 < y < L_y$, we multiply $d_i$ by the masking factor:

$$f = \frac{1}{2}\left\{1 + \tanh\left[-\alpha(r - r_0)\right]\right\}$$

In the examples presented in this paper $\alpha=12$, $r_0=1.75$, and the normalized coordinate $r$ is defined as follows:

$$r^2 = \left[(x - L_x/2)^2 + (y - L_y/2)^2\right]\frac{16}{L_x L_y} \quad \text{(non periodic problem)}$$

$$r = |y - L_y/2|\frac{4}{L_y} \qquad\qquad \text{(for problem periodic in x)}$$

The boundary conditions in the applications presented in the next three sections are thus appropriate for a $d_i=0$ (resistive MHD) plasma. They are of two types: periodic or conducting-wall. Let $\hat{n}$ be a unit vector normal to the wall and $\hat{t} \equiv \hat{n} \times \hat{z}$ be a unit vector in the tangential direction. Dirichlet boundary conditions for all the perturbed field quantities are applied at the wall. For example, for the poloidal flux: $\psi = \psi_t = \psi_{tt} = 0$. The same is true for $I$, $n$, $p_e$, $p$, and for the z-component of the velocity, $Vz$.. For the other velocity variables, we have for the stream function: $U = U_t = U_{tt} = U_{nn} = 0$, and for the potential: $\chi_n = \chi_{nt} = \chi_{nn} + \chi_{tt} = 0$.

## VIII: Plane Wave Propagation

As a first test we examine the ability to calculate small amplitude wave propagation parallel to the poloidal field. Taking the density to be uniform and the electron pressure to vanish, we linearize about an equilibrium with $I = I_0$, $\psi = \delta y$, $p = p_0$, where $I_0 = 1$, $\delta=0.1$, and $p_0=0.01$. This is meant to model the conditions in a low-beta tokamak plasma with propagation dominantly in the poloidal plane. In this case $I$ corresponds to the toroidal field and $\psi$ to the poloidal flux. Assuming sinusoidal variation in $x$ and $t$: $\sin(kx - \omega t)$, we find the following dispersion relation for the square of the frequency, $\Omega = \omega^2$:

$$\Omega^3 + A\Omega^2 + B\Omega + C = 0$$
$$A = -k^2\left[2\delta^2 + \gamma p_0 + I_0^2 + k^2\delta^2\right]$$
$$B = k^4\left[\delta^4 + \gamma p_0\left(2\delta^2 + k^2\delta^2\right) + \delta^2 I_0^2\right]$$
$$C = -k^6 \gamma p_0 \delta^4$$

(8.1)

Here $\gamma=5/3$ is the adiabatic index. For a particular value of $k=1, 2, ...$, we define a doubly periodic domain with $0 < x < 2\pi/k$ and $0 < y < 2\pi/k$ and initialize the perturbation to be one of the three roots of equation (8.1) corresponding to the (i) Slow , (ii) Alfven, or (iii) Fast branch, modified by the 2-fluid terms. We set $\psi = 10^{-4}$, and the other perturbed quantities are initialized as follows:

$$U = -(k/\omega)\delta\psi$$

$$I = \left[ \left( 1 - \frac{k^2\delta^2}{\omega^2} \right) - \frac{I_0^2}{\left( \omega^2/k^2 - \gamma p_0 \right)} \right]^{-1} (k^3/\omega)\delta\psi$$

$$V = -(k/\omega)\delta I \tag{8.2}$$

$$\chi = \frac{\omega I_0}{\left( \omega^2 - \gamma p_0 k^2 \right)} I$$

$$p = \gamma p_0 (k^2/\omega)\chi$$

We follow the evolution of the wave for the time $T = 2\pi k/\omega$ that it should theoretically take to traverse a single period, and compute the $L_2$ norm of the difference between the final and initial conditions, normalized to the initial amplitude. In the computational studies, we included small dissipative terms with amplitude $\kappa=\mu=\eta=4.\times10^{-5}$ for the fast wave initialization and $\kappa=\mu=\eta=4.\times10^{-4}$ for the Alfven and Slow wave initializations. We note that this will affect the minimum value of the error that can be obtained as these are not taken into account in the analytic dispersion relation. The arrangement of the triangular elements for the $4 \times 4$ case, and the initial 1D sinusoidal perturbation of the $\psi$ function are shown in Fig. 1.
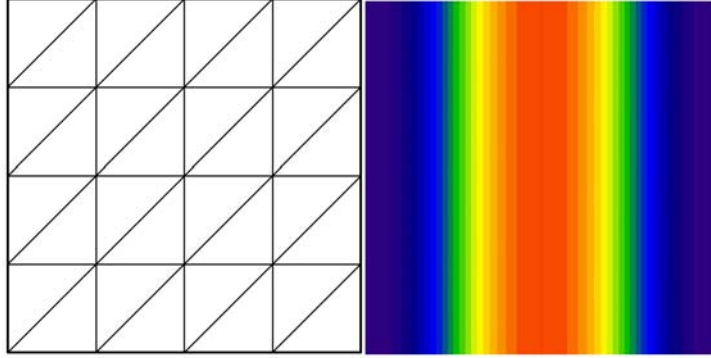


**Figure 1: Left shows arrangements of triangles for 4 x 4 doubly periodic wave propagation test. Right is corresponding initial contours of poloidal flux $\psi$.**

We plot the relative error in the plane wave convergence test for a particular wave number $k=1$ in Fig. 1 as a function of the time step used in the calculation. The solid (black) curve was initialized to an eigenmode of the Fast Wave with $\omega/k=1.018057$, the dashed (red) curve was initialized to the Alfven Wave with $\omega/k=0.100329$, and the dotted (blue) curve was initialized to the Slow Wave with $\omega/k=0.0126393$. For the Fast Wave we compute the $L_2$ error using the variable $I$, for the Alfven Wave we use $\psi$, and for the slow wave we use $p$. For the Fast wave we use an implicitness parameter of $\theta=0.51$, and for the Alfven and Slow wave we used $\theta=0.55$.
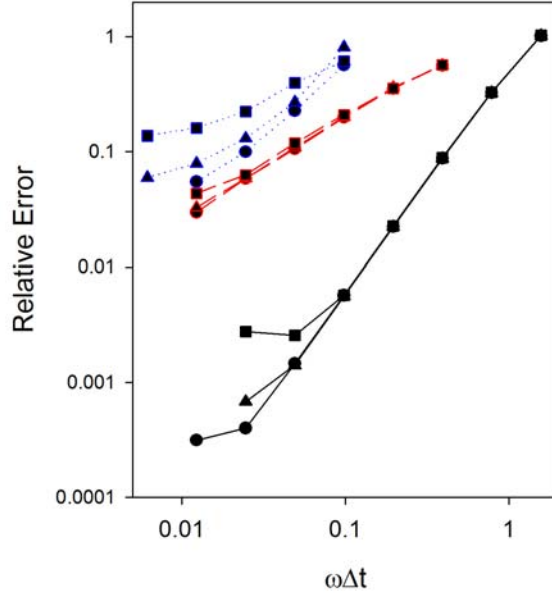
## Plane Wave Convergence Test



**Figure 2: (Color online) Relative error after propagation for one wavelength when periodic plasma is initialized in an eigenmode of one of the 3 waves for wave number *k=1*. The solid (black) curve was initialized to an eigenmode of the Fast Wave with *ω/k=1.018057*, the dashed (red) curve was initialized to the Alfven Wave with *ω/k=0.100329*, and the dotted (blue) curve was initialized to the Slow Wave with *ω/k=0.0126393*.Circles, triangles, and squares correspond to using 32, 8, and 4 triangles per linear wavelength.**

This is a very stringent test as it measures to what degree the initial state is a "pure" eigenmode in both space and time. The total $L_2$ error is the result of many factors: the propagation velocity is slightly off, the wave damps, or other eigenmodes get excited. We can see that the Fast Wave is converging most rapidly as both the time step and mesh spacing decreases. The sub-dominant waves also are converging, but more slowly.

## IX. The Tilting Cylinder

This problem, in the resistive (single fluid) MHD limit, was proposed in [16], and solutions for reduced MHD are given in [3] (2-field model) and [4] (4-field model). Following [16], we define an initial bipolar vortex equilibrium state:

$$\psi^0(x, y) = \begin{cases} [2/kJ(k)]J_1(kr)\cos\theta, & r < 1 \\ (r - 1/r)\cos\theta, & r > 1 \end{cases} \quad J_1(k) = 0. \tag{9.1}$$

We have defined a polar coordinate system such that $y = r\cos\theta$, $x = r\sin\theta$. For given values of the parameters $B_0$ and $\beta_P$, the initial longitudinal field and electron pressure inside the radius $r < 1$ are defined as:

21

$$\left[ I^0(x, y) \right]^2 = B_0^2 + (1 - \beta_P) k^2 \left[ \psi^0(x, y) \right]^2$$

$$p_e^0(x, y) = \frac{1}{2} k^2 \beta_P \left[ \psi^0(x, y) \right]^2 + 0.01$$

(9.2)

For $r > 1$, these are both constant so as to be continuous at $r=1$. The initial ion pressure and density are set to zero and unity, respectively. In these calculations we took the background field $B_0 = 1$. It is readily verified that this specification corresponds to a configuration satisfying the equilibrium equation: $\nabla p = \vec{J} \times \vec{B}$.

To illustrate the flexibility of this approach, we have perturbed the above equilibrium and computed the time evolution for several sets of equilibrium parameters corresponding to varying the quantity $\beta_P$ from zero to one, and varying the ion skin depth, to which the lengths are scaled. As an aid to doing this, we utilize the ion skin depth parameter $d_i$, discussed at the end of Section III. This appears such that when $d_i=1$ the ion skin depth is unity in these units, when $d_i=0.1$, it is $1/10^{th}$ unit, and when $d_i=0$, the ion skin depth shrinks to zero and the equations reduce to resistive MHD. We compute the linear growth rate by renormalizing the solution back to a fixed amplitude each timestep and computing the growth rate from the rate of change of the kinetic energy $K^n$: $\gamma = [K^{n+1}-K^n]/[\Delta t \times (K^{n+1}+K^n)]$. The values quoted are when this no longer changes with cycle number $n$.
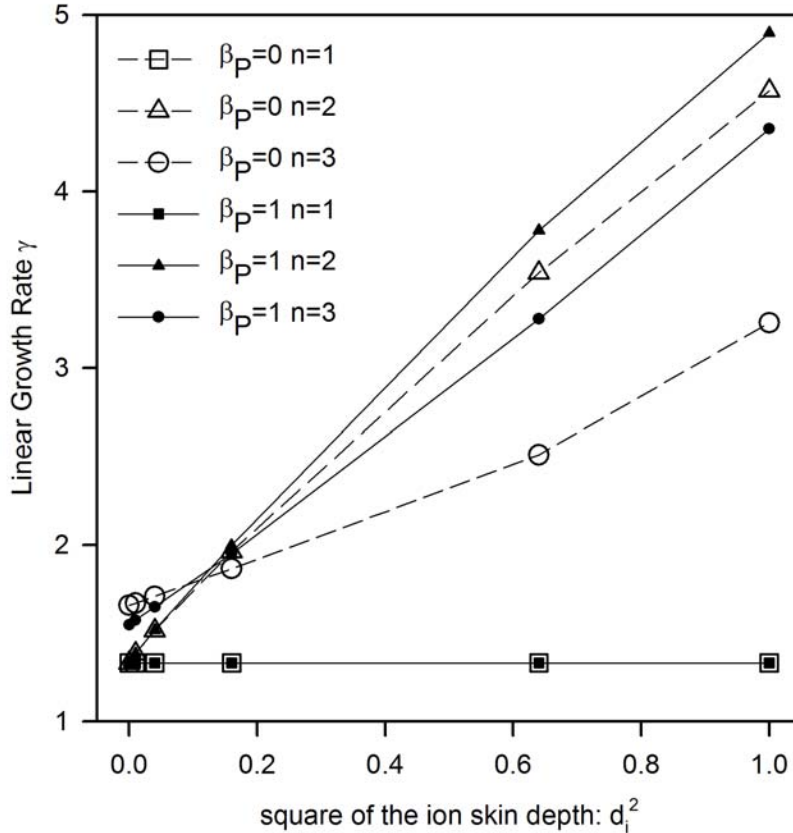


Figure 3: Growth rate vs ion skin depth for two equilibrium ($\beta_P=0$ and $\beta_P=1$) and for 3 sets of equations.

The results of this study are shown in Figures 3-4. The different curves in Figure 3 correspond to different sets of equations, and $\beta_P$ values of either zero or one. The curve $n=1$ corresponds to just one velocity variable, $U$, and one field variable, $\psi$. The curve $n=2$ adds the velocity variable $V_z$ and the field variable $I$, and the curve $n=3$ adds the velocity variable $\chi$ and the field variable $p_e$ to give the full system of equations discussed in this paper. The curves corresponding to $n=1$ and $n=2$ were discussed in [3] and [4]. These were computed in our formulation by keeping just the upper left element and the upper $2 \times 2$ sub-matrix in our equations (4.15) and (5.3).
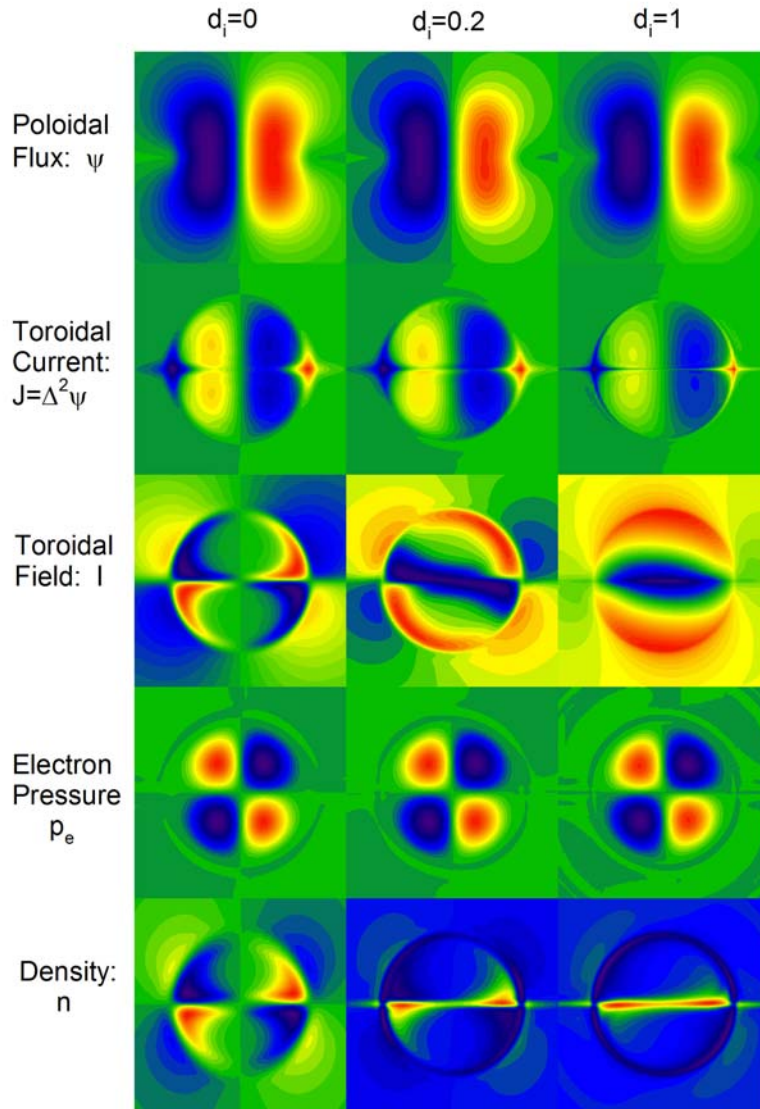


**Figure 4a: (Color online) Linear eigenfunctions of the field variables for beta=1 configurations for several values of $d_i$.**
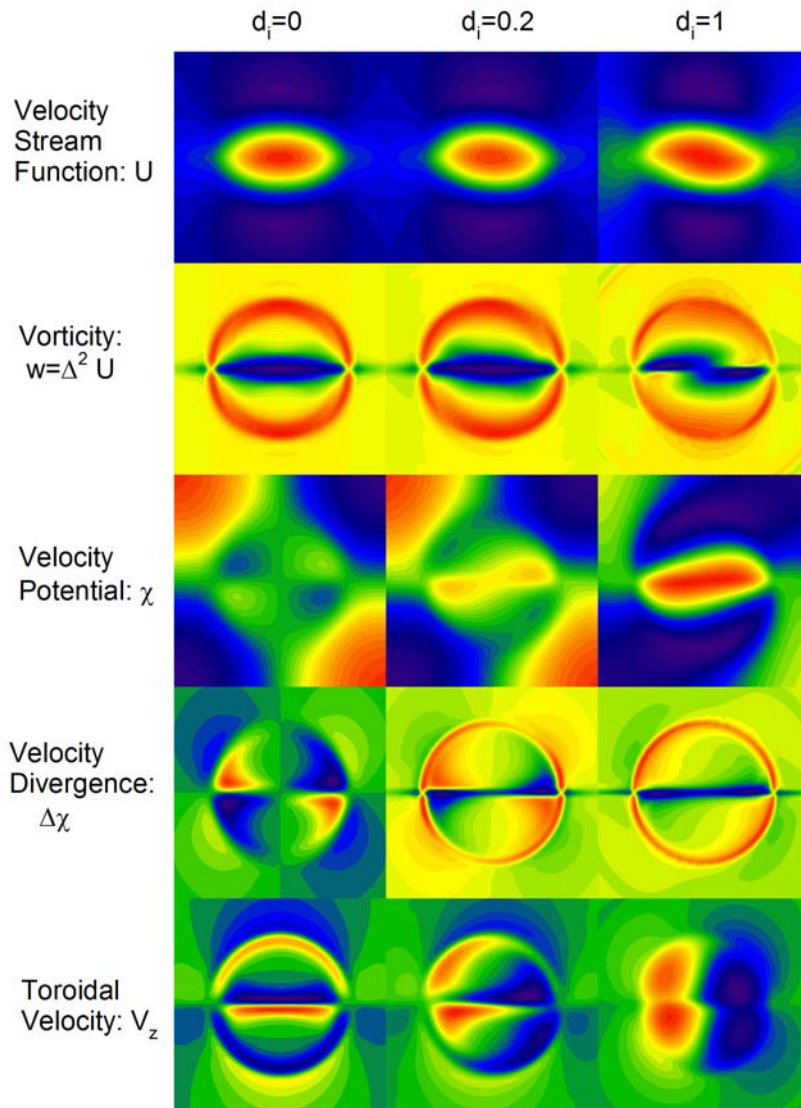
**Figure 4b: (Color online) Linear eigenfunctions of the velocity variables for beta=1 configurations for several values of $d_i$.**

We see from Figure 3 that except for the n=1 reduced model, the linear growth rate increases significantly as the ion skin depth becomes comparable to the equilibrium scale length. The n=2 reduced model gives the correct qualitative behavior, but can be substantially off in the actual growth rate.

To illustrate the complexity of the linear eigenfunction and how it changes with the ion skin depth, we show five of the field variables and five of the velocity variables in Figures 4a and 4b for several configurations corresponding to $\beta_P=1$ and scanning several values of $d_i$. Note that only 7 independent scalar variables are being integrated in time in this example (since the ion pressure is zero). While we have plotted the toroidal current density, the vorticity, and the velocity divergence, these are not independently time-advanced variables, but are

obtained by taking the Laplacian of the poloidal flux $\psi$, the velocity stream function $U$, and the velocity potential $\chi$, respectively.

These growth rates were obtained using a uniformly laid-out triangular mesh such as shown in Fig 1a. The baseline calculations were done with a mesh of $51 \times 51$ nodes and a timestep of $\Delta t=0.05$. We find that the growth rates typically change only in the $4^{\text{th}}$ decimal place when repeating the calculation on a mesh with *101 × 101* nodes, and in the $3^{\text{rd}}$ decimal place when increasing the timestep to $\Delta t=0.10$

## X. A Reconnection Problem

What has become a "standard problem" in 2-fluid magnetic reconnection was proposed in [17]. We define an initial equilibrium as follows;

$$\psi^0(x,y) = \frac{1}{2}\ln\left(\cosh 2y\right)$$

$$I^0(x,y) = 0$$

$$P^0(x,y) = \left[\sec h^2(2y)+0.2\right] \tag{10.1}$$

$$n^0(x,y) = \left[\sec h^2(2y)+0.2\right]$$

$$P_e^0(x,y) = 0.2P^0(x,y)$$

All other quantities are initialized to zero. A perturbation is applied at time *t=0* as follows:

$$\psi(x,y) = \varepsilon \cos k_x x \cos k_y y . \tag{10.2}$$

The initial equilibrium and perturbed current densities are just the Laplacian of the fluxes, $J^0 = \nabla^2\psi^0, J = \nabla^2\psi$. The computation is carried out in a rectangular domain: $-L_x/2 \le x \le L_x/2$ and $-L_y/2 \le y \le L_y/2$. The system is taken to be periodic in the $x$-direction with ideal conducting boundaries at $y = \pm L_y/2$. The parameters are chosen such that $k_x = 2\pi/L_x$, $k_y = \pi/L_y$, with $L_x = 25.6, L_y = 12.8,$ and $\varepsilon = 0.1$.

These calculations used values of resistivity $\eta = 0.005$, viscosities $\mu=\mu_C=0.05$, and thermal conductivity $\kappa=0.02$. An implicitness parameter of $\theta=0.51$ was used. For all calculations presented, the time step used was as follows: From t=0 to t=20, $\Delta t=0.2$; from t=20 to t=24, $\Delta t=0.1$; from t=24 to t=34, $\Delta t=0.05$; from t=34 to t=40, $\Delta t=0.1$. These timesteps were chosen for accuracy considerations and were the same for all spatial resolutions. There were a total of 400 timesteps for each calculation.

We performed a series of calculations with N×N equally spaced nodes with N=61, 91, 121, and 151. The triangular elements were then constructed by inserting diagonals similar to

what was shown in Fig. 1. The inter-node spacing in the x-direction is denoted by Δx. This enters into the coefficients for the hyper-resistivity, equation (2.5), which we define as follows: $\lambda=C_H h^2$, where $h$ is a typical triangle dimension and with the coefficient $C_H=1.0$ used in these calculations. Since the physical value of the hyper-resistivity is smaller than any of those used in this series, the meaningful result is to perform a convergence study and take the limit of $h \rightarrow 0$. The reason for choosing this dependency of $\lambda$ on $h$ is discussed below.

.



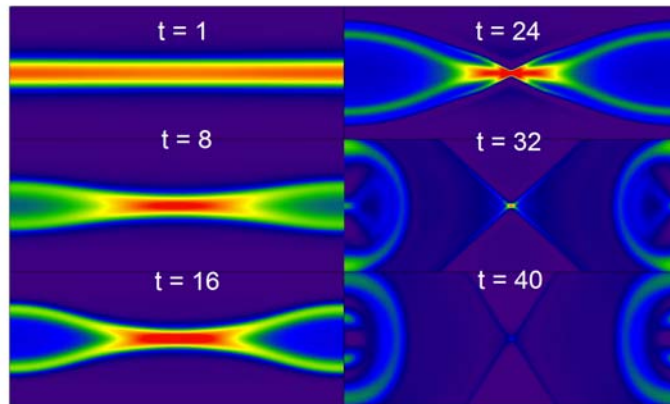**Figure 5: (Color online) Contours of the toroidal current density at selected times. Note that a transition occurs between the time of t=16 and t=32.**
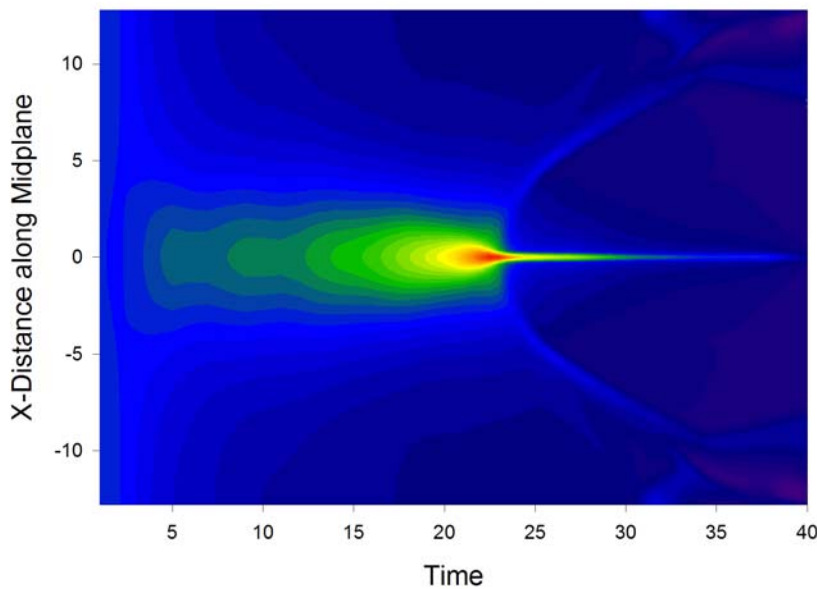


**Figure 6: (Color online) Midplane Current density vs time. Vertical axis is current density along midplane y=0, and horizontal axis is time. Note the abrupt transition at t ~ 24.**

We show typical results for contours of the toroidal current density, $J = \nabla^2 \psi$, for the 121 × 121 nonlinear calculation at selected times in Figure 5. We note that a transition occurs around the time t=24, at which time the current density abruptly peaks on axis. To illustrate this more clearly, we show in Figure 6 a plot of the current density along the y=0 midplane as a function of the horizontal (x) distance and time. It can be seen from this graph how rapidly the transition occurs at time t~24.

To understand this transition better, we plot in Figure 7 the z-component of the electric field along the midplane, *y=0,* at two times: *t=20* (before the transition) and *t=30* (after the transition). The total electric field is the smooth dark black line in Figure 7. It is seen from equation (2.1f) that this is made up of several different contributions. For convenience, we rewrite the z component of equation (2.1f) here:

$$\hat{z} \cdot \vec{E} = \frac{1}{ne} \hat{z} \cdot \vec{J} \times \vec{B} - \hat{z} \cdot \vec{V} \times \vec{B} + \eta \hat{z} \cdot \vec{J} - C_H \eta h^2 \nabla^2 \hat{z} \cdot \vec{J} \qquad (10.3)$$
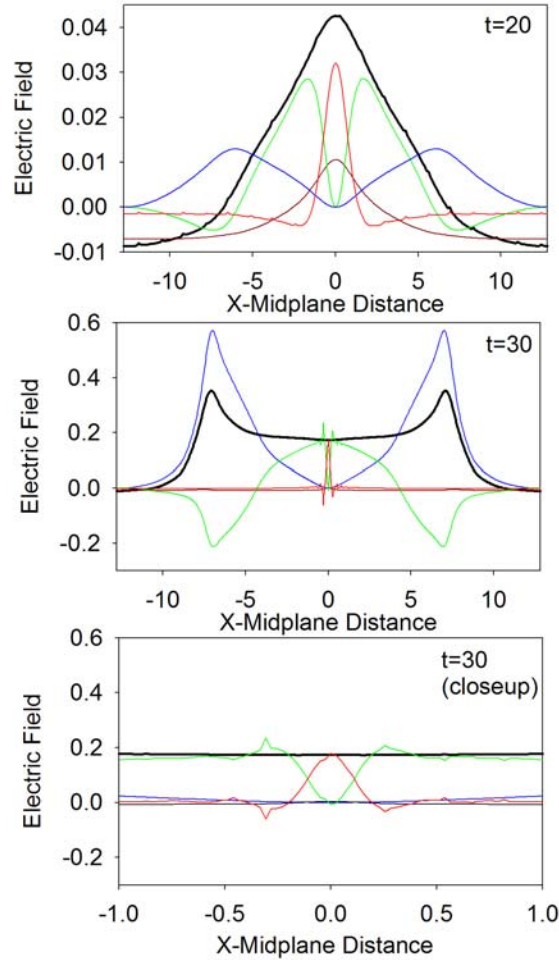


**Figure 7: (Color online) Different components of the Electric Field. Solid black line is the total electric field. Green line is part due to J × B term, blue to the V × B term, dark red to the resistive term, and the bright red to the hyper-resistive term. Top figure is before transition, middle is after transition, and bottom is close-up of middle figure.**

The terms in equation (10.3) are written in the order in which they occur when traversing down a vertical line in Fig. 7a (top) at the location x=10. The top, bold curve is the total electric field. The next curves are the field due to the $J \times B$ term, the $V \times B$ term, the resistive term, and the hyper-resistive term. We can see from Fig. 7b (middle) that at time t=30, after the transition, the $J \times B$ is the only significant contribution to the electric field in the vicinity of the x-point (central location), but that it must vanish exactly at the x-point since the

.



**Figure 8: Top figure is global kinetic energy vs time for 4 calculations with differing resolution, middle figure is the flux change at the midpoint vs time, and bottom graph is the time derivative of the middle curves. Reconnected Flux (middle curves) at time t=40 is seen to be converging to a unique value.**

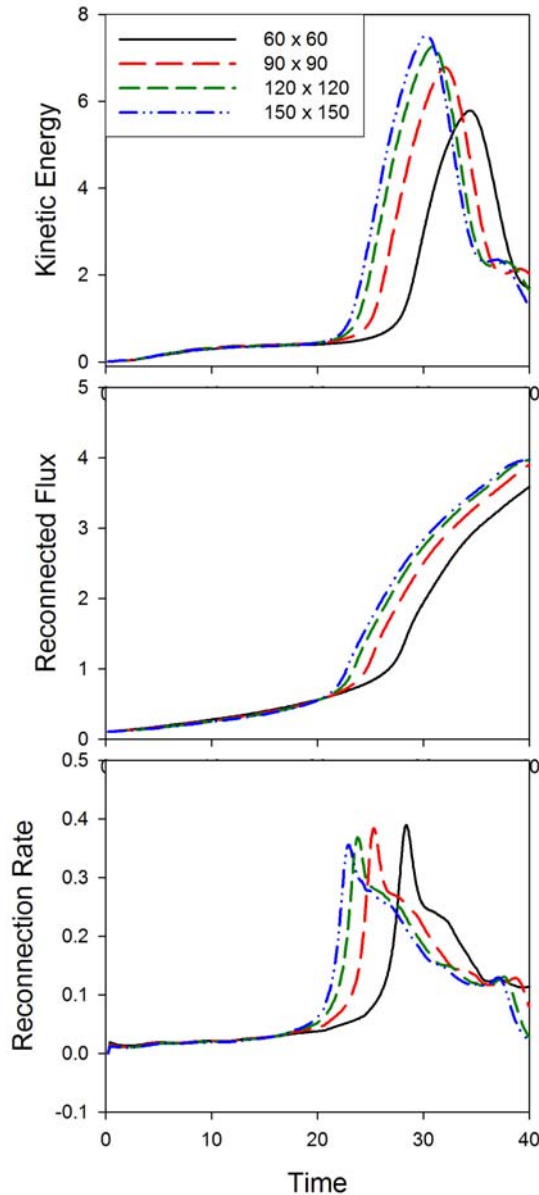magnetic field vanishes there (B=0). In Fig. 7c (bottom), which is a blowup of Fig. 7b, we see that in the very near vicinity of the x-point, the term due to the hyper-resistivity becomes important. The scaling factor of $h^2$ was, in fact, chosen so that there would always be several triangular elements within this transition region. It has been shown previously that this leads to a globally convergent result in the limit as $1/N \sim h \rightarrow 0$. [18]

Finally, we show in Figure 8 some results comparing the series of calculation with everything else the same but different spatial resolutions (different number of elements). These graphs show both what stringent resolution requirements this problem has, and that the global quantities are converging, although slowly. We postulate that the slow convergence is due to the singular nature of the current sheet after the transition.

The time advance equations are not written in conservation form, although they should conserve energy as discussed following Equation (2.3). We find that the numerical results conserve global energy to better than 1 part in $10^3$ throughout the 120×120 calculation, and that this relative error decreases for the better resolved calculations

## X. Summary and Future Directions

We have described a method for solving a high-order set of partial differential equations providing a two-fluid description of a high temperature magnetized plasma in a relatively simple geometry and in 2D. The flux function/potential representation of the vector velocity and magnetic fields leads to a representation in which the divergence of the magnetic field is intrinsically zero, and which allows accurate computation of nearly incompressible flow fields.

As discussed in [3], the technique should compare favorably with other finite element based methods in 2D. The fact that all the DOF are located at the nodes and are shared by all the surrounding triangles leads to a very compact representation. The $C^l$ continuity property allows computation with spatial operators containing up to 4th order derivatives without introducing new auxiliary variables. A split semi-implicit method is used that breaks the full time advance into four sequential time advances, each involving smaller matrices. These features make feasible direct solution of the resulting sparse matrix equations, avoiding the slow convergence problems that would result if an iterative method were applied to these multiscale equations.

Illustrative examples are given of plane wave propagation, the computation of linear eigenmodes of a tilting cylinder, and a challenging problem in magnetic reconnection. Earlier studies have also demonstrated the applicability of this technique to the gravitational instability [13].

Work is presently underway to extend this work in several directions. It is being extended to cylindrical geometry in order to be applicable to an axisymmetric torus. An adaptive algorithm is being implemented to allow concentration of nodes in regions of high gradients. Three-dimensional extensions are being considered where the third dimension is represented

by finite differences or by a spectral expansion.  Indications are that the techniques demonstrated here form a powerful base that can be extended into more complex geometries.

**Acknowledgments**

## Appendix A:  Definitions of the operators

I.  Operators with 2 indices:

$$A_{i,j}U_j \equiv \iint v_i \nabla^2 U d\xi d\eta$$

$$B_{i,j}U_j \equiv \iint v_i \nabla^4 U d\xi d\eta$$

$$D_{i,j}U_j \equiv \iint v_i U d\xi d\eta$$

$$X_{i,j}^0 N_j \equiv \iint v_i n_x d\xi d\eta$$

$$Y_{i,j}^0 N_j \equiv \iint v_i n_y d\xi d\eta$$

II. Operators with 3 indices:

$$K_{i,j,k}\Psi_j U_k \equiv \iint v_i [\psi, U] d\xi d\eta = -K_{i,k,j}\Psi_j U_k$$

$$K_{i,j,k}^1 \Psi_k U_j \equiv \iint v_i \psi U d\xi d\eta = K_{i,k,j}^1 \Psi_k U_j$$

$$K_{i,j,k}^2 N_k V_j \equiv \iint (v_i n, V_z) d\xi d\eta$$

$$G_{i,j,k}\Psi_j U_k \equiv \iint v_i \left[\nabla^2 \psi, U\right] d\xi d\eta = -\iint \nabla^2 \psi [v_i, U] d\xi d\eta$$

$$G_{i,j,k}^2 N_k \dot{U}_j \equiv -\iint n(v_i, \dot{U}) d\xi d\eta$$

$$G_{i,j,k}^3 U_j N_k \equiv \iint v_i \left\{ -n\nabla^4 U - (n, \nabla^2 U) \right\} d\xi d\eta = -\iint \nabla^2 U \nabla \cdot (n\nabla v_i) d\xi d\eta$$

$$G_{i,j,k}^4 \Psi_j \Psi_k \equiv \iint \nabla^2 \psi (v_i, \psi) d\xi d\eta$$

$$G_{i,j,k}^5 I_j I_k \equiv -\iint v_i \tfrac{1}{2} \nabla^2 I^2 d\xi d\eta = \iint I(I, v_i) d\xi d\eta$$

$$G_{i,j,k}^{6A} \dot{X}_j P_k \equiv -\iint (v_i, (p, \dot{\chi})) d\xi d\eta$$

$$G_{i,j,k}^{6B} \dot{X}_j P_k \equiv \iint p\nabla^2 \dot{\chi} \nabla^2 v_i d\xi d\eta$$

$$G_{i,j,k}^7 \dot{U}_j P_k \equiv -\iint (v_i, [p, \dot{U}]) d\xi d\eta$$

$$G_{i,j,k}^{12} I_j I_k \equiv \iint v_i \left( I_{xx}^2 + I_{yy}^2 + 2I_{xy}^2 \right) d\xi d\eta$$

$$G_{i,j,k}^{13} E_k P_j \equiv \iint v_i \nabla^4 (pE) d\xi d\eta = \iint \nabla^2 v_i \nabla^2 (pE) d\xi d\eta$$

$$G^{14}_{i,j,k}U_jU_k \equiv \iint \nu_i \left\{ \left( U_{yy} - U_{xx} \right)^2 + 4U_{xy}^2 \right\} d\xi d\eta$$

$$G^{15}_{i,j,k}X_jX_k \equiv \iint \nu_i \left( 4\chi_{xy}^2 - 4\chi_{xx}\chi_{yy} + 2\left| \nabla^2 \chi \right|^2 \right) d\xi d\eta$$

$$G^{16}_{i,j,k}U_jX_k \equiv \iint \nu_i 4\left\{ U_{xy} \left( \chi_{xx} - \chi_{yy} \right) + \chi_{xy} \left( U_{yy} - U_{xx} \right) \right\} d\xi d\eta$$

$$G^{17}_{i,j,k}X_jX_k \equiv \iint \nu_i \left| \nabla^2 \chi \right|^2 d\xi d\eta$$

$$H^3_{i,j,k}S_{\psi k}\Psi_j \equiv \iint \left\{ -J\left( \nu_i, S_\psi \right) - \nabla^2 S_\psi \left( \nu_i, \psi \right) \right\} d\xi d\eta$$

$$H^5_{i,j,k}S_{Ik}I_j \equiv \iint \left\{ -I\left( \nu_i, S_I \right) - S_I \left( I, \nu_i \right) \right\} d\xi d\eta$$

$$X^1_{i,j,k}N_kU_j \equiv \iint \nu_i \left[ n, U \right]_x d\xi d\eta$$

$$X^2_{i,j,k}N_kX_j \equiv \iint \nu_i \left[ (n, \chi) + n\nabla^2 \chi \right]_x d\xi d\eta$$

$$Y^1_{i,j,k}N_kU_j \equiv \iint \nu_i \left[ n, U \right]_y d\xi d\eta$$

$$Y^2_{i,j,k}N_kX_j \equiv \iint \nu_i \left[ (n, \chi) + n\nabla^2 \chi \right]_y d\xi d\eta$$

### III. Operators with 4 indices:

$$V^1_{i,j,k,l}N_lU_kU_j = V^2_{i,k,j,l}N_lU_kU_j \equiv \iint \left\{ -n\nabla^2 U \left[ \nu_i, U \right] + \tfrac{1}{2} n \left[ \nu_i, (U, U) \right] \right\} d\eta d\xi$$

$$V^3_{i,j,k,l}N_lX_kU_j = V^4_{i,k,j,l}N_lX_kU_j \equiv \iint \nu_i \left\{ -n\nabla^2 U \left( \nu_i, \chi \right) + \left[ n, \nu_i \right] \left[ \chi, U \right] \right\} d\eta d\xi$$

$$V^5_{i,j,k,l}N_lX_kX_j = V^6_{i,k,j,l}N_lX_kX_j \equiv -\tfrac{1}{2} \iint \nu_i \left[ n, (\chi, \chi) \right] d\eta d\xi$$

$$V^7_{i,j,k,l}N_lU_kV_{zj} = V^8_{i,k,j,l}N_lU_kV_{zj} \equiv \iint \nu_i n \left[ V_z, U \right] d\xi d\eta$$

$$V^9_{i,j,k,l}N_lX_kV_{zj} = V^{10}_{i,k,j,l}N_lX_kV_{zj} \equiv \iint \nu_i n \left( V_z, \chi \right) d\xi d\eta$$

$$V^{11}_{i,j,k,l}N_lU_kX_j = V^{12}_{i,k,j,l}N_lU_kX_j \equiv \iint \left\{ -n\nabla^2 U \left[ \nu_i, \chi \right] - n \left( \nu_i, \left[ \chi, U \right] \right) \right\} d\eta d\xi$$

$$V^{13}_{i,j,k,l}N_lX_kX_j = V^{14}_{i,k,j,l}N_lX_kX_j \equiv -\tfrac{1}{2} \iint n \left( \nu_i, (\chi, \chi) \right) d\eta d\xi$$

$$V^{15}_{i,j,k,l}N_lU_kU_j = V^{16}_{i,k,j,l}N_lU_kU_j \equiv \iint \left\{ n\nabla^2 U \left( \nu_i, U \right) - \tfrac{1}{2} n \left( \nu_i, (U, U) \right) \right\} d\eta d\xi$$

$$C^1_{i,j,k,l}\Psi_k\Psi_l\dot{U}_j \equiv \nabla^2 \psi \left[ \left[ \psi, \dot{U} \right], \nu_i \right] + \left( \left[ \psi, \dot{U} \right], \left[ \nu_i, \psi \right] \right)$$

$$C^3_{i,j,k,l}\Psi_k\Psi_l\dot{X}_j \equiv \nabla^2 \psi \left[ (\psi, \dot{\chi}), \nu_i \right] + \left( (\psi, \dot{\chi}), \left[ \nu_i, \psi \right] \right)$$

$$C^5_{i,j,k,l}I_l\Psi_k\dot{U}_j = -\left[ \psi, \dot{U} \right] \left[ \nu_i, I \right] + \left[ I, \dot{U} \right] \left[ \nu_i, \psi \right]$$

$$C^7_{i,j,k,l}I_l\Psi_k\dot{X}_j = -(\psi, \dot{\chi}) \left[ \nu_i, I \right] + (I, \dot{\chi}) \left[ \nu_i, \psi \right] + I\nabla^2 \dot{\chi} \left[ \nu_i, \psi \right]$$

$$C^9_{i,j,k,l}\psi_l\psi_k\dot{V}_j = -\left[ \psi, V_j \right] \left[ \psi, \nu_i \right]$$

$$C_{i,j,k,l}^{11} \Psi_l \Psi_k \dot{U}_j = -\left( (v_i, \psi), [\psi, \dot{U}] \right) + \nabla^2 \psi \left( v_i, [\psi, \dot{U}] \right)$$

$$C_{i,j,k,l}^{13} \dot{X}_j \Psi_k \Psi_l = -\left( (v_i, \psi), (\psi, \dot{\chi}) \right) + \nabla^2 \psi \left( v_i, (\psi, \chi) \right)$$

$$C_{i,j,k,l}^{15} \dot{V}_j \Psi_k I_l = -I \left[ \psi, \dot{V} \right] \nabla^2 v_i$$

$$C_{i,j,k,l}^{17} \dot{X}_j I_k I_l = -I \left[ I \nabla^2 \dot{\chi} + (I, \dot{\chi}) \right] \nabla^2 v_i$$

$$U_{i,j,k,l}^1 E_l \Psi_j \Psi_k = U_{i,k,j,l}^2 E_l \Psi_j \Psi_k = -\iint \nabla^2 \Psi E [v_i, \Psi] d\xi d\eta$$

$$U_{i,j,k,l}^3 E_l \Psi_j I_k = U_{i,k,j,l}^4 E_l \Psi_j I_k = \iint v_i E [\Psi, I] d\xi d\eta$$

$$U_{i,j,k,l}^5 E_l P_{ej} I_k = U_{i,k,j,l}^6 E_l P_{ej} I_k = \iint v_i P_e [E, I] d\xi d\eta$$

# Appendix B:  Computation of the Operators:

Each of the scalar variables is expanded within each element as a sum over the 18 basis functions, for example as given in equation (3.2).  Each basis function is a quintic polynomial in the local triangle coordinates given in [3], i. e.

$$v_j \equiv \sum_{i=1}^{20} g_{i,j} \xi^{m_i} \eta^{n_i} \tag{B.1}$$

To obtain the form of the operators, we expand all variables in tis polynomial representation and apply the operation and integrations in the local coordinates.  Thus, for example,

$$
\begin{aligned}
A_{i,j}\Phi_j &\equiv \iint v_i(\xi,\eta)\nabla^2\phi(\xi,\eta)d\xi d\eta \\
&= -\iint \nabla v_i(\xi,\eta)\cdot\nabla\phi(\xi,\eta)d\xi d\eta \\
&= -\sum_{p=1}^{20}\sum_{q=1}^{20}\sum_{j=1}^{18} g_{p,i}g_{q,j}\left[ m_p m_q \iint \xi^{m_p+m_q-2}\eta^{n_p+n_q}d\xi d\eta + n_p n_q \iint \xi^{m_p+m_q}\eta^{n_p+n_q-2}d\xi d\eta \right]
\end{aligned}
\tag{B.2}
$$

where $g_{p,i}$ is the geometry matrix defined in [3] and the integrals over the triangle are evaluated in closed form.  In the concise notation that follows, we will write this as:

$$A_{i,j}\Phi_j = -[m_p m_q F(-2,0) + n_p n_q F(0,-2)]. \tag{B.3}$$

The summations, the multiplication by the appropriate geometry matrices, and the integrals involving the $m_i$ and $n_i$ are implied.  The other operators are computed similarly, using the same notation.

$$
\begin{aligned}
B_{i,j} &= m_p(m_p-1)m_q(m_q-1)\times F(-4,0) + n_p(n_p-1)n_q(n_q-1)\times F(0,-4) \\
&\quad + [m_p(m_p-1)n_q(n_q-1) + m_q(m_q-1)n_p(n_p-1)]\times F(-2,-2)
\end{aligned}
$$

$$D_{i,j} = F(0,0)$$

$$X_{i,j}^0 = \cos\theta m_q F(-1,0) - \sin\theta n_q F(0,-1)$$

$$Y_{i,j}^0 = \sin\theta m_q F(-1,0) + \cos\theta n_q F(0,-1)$$

$$K_{i,j,k} = \left(m_q n_r - m_r n_q\right) F\left(m_p + m_q + m_r - 1, n_p + n_q + n_r - 1\right)$$

$$K_{i,j,k}^1 = F(0,0)$$

$$K_{i,j,k}^2 = \left(m_p + m_r\right)m_q F\left(-2,0\right) + \left(n_p + n_r\right)n_q F\left(-2,0\right)$$

$$G_{i,j,k} = -\left(m_p n_r - m_r n_p\right)\left[ m_q\left(m_q-1\right)F\left(-3,-1\right) + n_q\left(n_q-1\right)F\left(-1,-3\right)\right]$$

$$G_{i,j,k}^2 = -\left[ m_p m_q F\left(-2,0\right) + n_p n_q F\left(0,-2\right)\right]$$

$$G_{i,j,k}^{3} = \left[ m_p m_q (m_q - 1)(m_p + m_r - 1) \right] F(-4,0) + \left[ n_p n_q (n_q - 1)(n_p + n_r - 1) \right] F(0,-4)$$
$$+ \left[ n_p m_q (m_q - 1)(n_p + n_r - 1) + m_p n_q (n_q - 1)(m_p + m_r - 1) \right] F(-2,-2)$$

$$G_{i,j,k}^{4} = m_q \left( m_q - 1 \right) m_p m_r F(-4,0) + n_q \left( n_q - 1 \right) n_p n_r F(0,-4)$$
$$+ \left[ m_q \left( m_q - 1 \right) n_p n_r + n_q \left( n_q - 1 \right) m_p m_r \right] F(-2,-2)$$

$$G_{i,j,k}^{5} = m_p m_r F(-2,0) + n_p n_r F(0,-2)$$

$$G_{i,j,k}^{6} = \left[ m_p m_q \{ -m_r (m_r + m_q - 2) + \gamma (m_q - 1)(m_p - 1) \} \right] F(-4,0)$$
$$+ \left[ \begin{array}{l} + m_p n_q \{ -n_r (m_r + m_q) + \gamma (n_q - 1)(m_p - 1) \} \\ + n_p m_q \{ -m_r (n_r + n_q) + \gamma (m_q - 1)(n_p - 1) \} \end{array} \right] F(-2,-2)$$
$$+ \left[ n_p n_q \{ -n_r (n_r + n_q - 2) + \gamma (n_q - 1)(n_p - 1) \} \right] F(0,-4)$$

$$G_{i,j,k}^{7} = -(m_r n_q - m_q n_r) \left[ m_p (m_r + m_q - 1) \times F(-3,-1) + n_p (n_r + n_q - 1) \times F(-1,-3) \right]$$

$$G_{i,j,k}^{12} = m_q \left( m_q - 1 \right) m_r \left( m_r - 1 \right) \times F(-4,0) + 2 m_q m_r n_q n_r \times F(-2,-2)$$
$$+ n_q \left( n_q - 1 \right) n_r \left( n_r - 1 \right) \times F(0,-4)$$

$$G_{i,j,k}^{13} = \left( m_q + m_r \right) \left( m_q + m_r - 1 \right) m_p \left( m_p - 1 \right) \times F(-4,0)$$
$$+ \left[ \begin{array}{l} \left( m_q + m_r \right) \left( m_q + m_r - 1 \right) n_p \left( n_p - 1 \right) \\ + \left( n_q + n_r \right) \left( n_q + n_r - 1 \right) m_p \left( m_p - 1 \right) \end{array} \right] \times F(-2,-2)$$
$$+ \left( n_q + n_r \right) \left( n_q + n_r - 1 \right) n_p \left( n_p - 1 \right) \times F(0,-4)$$

$$G_{i,j,k}^{14} = m_q \left( m_q - 1 \right) m_r \left( m_r - 1 \right) F(-4,0) + n_q \left( n_q - 1 \right) n_r \left( n_r - 1 \right) F(0,-4)$$
$$+ \left[ -n_q \left( n_q - 1 \right) m_r \left( m_r - 1 \right) - m_q \left( m_q - 1 \right) n_r \left( n_r - 1 \right) + 4 m_q n_q m_r n_r \right] F(-2,-2)$$

$$G_{i,j,k}^{15} = 2 \left[ m_q \left( m_q - 1 \right) m_r \left( m_r - 1 \right) F(-4,0) + n_q \left( n_q - 1 \right) n_r \left( n_r - 1 \right) F(0,-4) + 2 m_q n_q m_r n_r F(-2,-2) \right]$$

$$G_{i,j,k}^{16} = 4 m_q m_r \left[ n_q \left( m_r - 1 \right) - n_r \left( m_q - 1 \right) \right] F(-3,-1) - 4 n_q n_r \left[ m_q \left( n_r - 1 \right) - m_r \left( n_q - 1 \right) \right] F(-1,-3)$$

$$G_{i,j,k}^{17} = m_q (m_q - 1) m_r (m_r - 1) F(-4,0) + n_q (n_q - 1) n_r (n_r - 1) F(0,-4)$$
$$+ \left[ m_q (m_q - 1) n_r (n_r - 1) + n_q (n_q - 1) m_r (m_r - 1) \right] F(-2,-2)$$

$$H^3_{i,j,k} = -m_p m_q m_r (m_r + m_q - 2) F(-4,0) - n_p n_q n_r (n_r + n_q - 2) F(0,-4)$$
$$- \left[ m_q n_r \left( m_p (n_r - 1) + n_p (m_q - 1) \right) + n_q m_r \left( n_p (m_r - 1) + m_p (n_q - 1) \right) \right] F(-2,-2)$$

$$H^5_{i,j,k} = -m_p (m_r + m_q) F(-2,0) - n_p (n_r + n_q) F(0,-2)$$

$$X^1_{i,j,k} = (m_q n_r - m_r n_q) \left[ m_p \cos \theta F(-2,-1) + n_p \sin \theta F(-1,-2) \right]$$

$$X^2_{i,j,k} = -m_q (m_r + m_q - 1) \left[ m_p \cos \theta F(-3,0) - n_p \sin \theta F(-2,-1) \right]$$
$$- n_q (n_r + n_q - 1) \left[ m_p \cos \theta F(-1,-2) - n_p \sin \theta F(0,-3) \right]$$

$$Y^1_{i,j,k} = (m_q n_r - m_r n_q) \left[ m_p \sin \theta F(-2,-1) + n_p \cos \theta F(-1,-2) \right]$$

$$Y^2_{i,j,k} = -m_q (m_r + m_q - 1) \left[ m_p \sin \theta F(-3,0) + n_p \cos \theta F(-2,-1) \right]$$
$$- n_q (n_r + n_q - 1) \left[ m_p \sin \theta F(-1,-2) + n_p \cos \theta F(0,-3) \right]$$

$$V^1_{i,j,k,l} = \left[ \begin{array}{l} m_q \left\{ m_r \left[ (m_q - 1)(n_s + n_p) - n_q m_s \right] - n_r m_p (m_q - 1) \right\} \times F(-3,-1) \\ + n_q \left\{ m_r n_p (n_q - 1) + n_r \left[ m_q n_s - (n_q - 1)(m_s + m_p) \right] \right\} \times F(-1,-3) \end{array} \right]$$

$$V^3_{i,j,k,l} = \left\{ \begin{array}{l} \left[ -m_r m_p m_q (m_q - 1) \right] F(-4,0) \\ + \left\{ \begin{array}{l} m_r n_q \left[ (m_r + m_q - 1)n_s - (n_q - 1)(m_s + m_p) - m_s n_r \right] \\ + n_r m_q \left[ (n_r + n_q - 1)m_s - (m_q - 1)(n_s + n_p) - n_s m_r \right] \end{array} \right\} F(-2,-2) \\ + \left[ -n_r n_p n_q (n_q - 1) \right] F(0,-4) \end{array} \right\}$$

$$V^5_{i,j,k,l} = \tfrac{1}{2} (m_s n_p - m_p n_s) \left[ m_r m_q F(-3,-1) + n_r n_q F(-1,-3) \right]$$

$$V^7_{i,j,k,l} = \left[ m_q n_r - m_r n_q \right] F(-1,-1)$$

$$V^9_{i,j,k,l} = \left[ m_q m_r F(-2,0) + n_q n_r F(0,-2) \right]$$

$$V^{11}_{i,j,k,l} = \left\{ \begin{array}{l} - \left[ (m_p n_q - m_q n_p) m_r (m_r - 1) + (m_q n_r - m_r n_q) m_p (m_q + m_r - 1) \right] F(-3,-1) \\ - \left[ (m_p n_q - m_q n_p) n_r (n_r - 1) + (m_q n_r - m_r n_q) n_p (n_q + n_r - 1) \right] F(-1,-3) \end{array} \right\}$$

$$V^{13}_{i,j,k,l} = \left\{ \begin{array}{l} \tfrac{1}{2} m_p m_q m_r (m_p + m_s - 1) F(-4,0) \\ + \tfrac{1}{2} \left[ \begin{array}{l} m_p n_q n_r (m_p + m_s - 1) \\ + n_p m_q m_r (n_p + n_s - 1) \end{array} \right] F(-2,-2) \\ + \tfrac{1}{2} n_p n_q n_r (n_p + n_s - 1) F(0,-4) \end{array} \right\}$$

$$V_{i,j,k,l}^{15} = \left\{ \begin{array}{l} \left[ -\tfrac{1}{2} m_p m_r m_q (m_r - m_q) \right] F(-4,0) \\[6pt] + \left[ \begin{array}{l} m_p m_r n_q (n_q - 1) + n_p n_r m_q (m_q - 1) \\ -\tfrac{1}{2} m_p n_r n_q \left( m_r + m_q \right) - \tfrac{1}{2} n_p m_r m_q \left( n_r + n_q \right) \end{array} \right] F(-2,-2) \\[12pt] + \left[ -\tfrac{1}{2} n_p n_r n_q \left( n_r - n_q \right) \right] F(0,-4) \end{array} \right\}$$

$$C_{i,j,k,l}^{1} = (m_s n_q - m_q n_s) \times \left\{ \begin{array}{l} \left[ \begin{array}{l} m_r(m_r - 1)\left[ (m_s + m_q - 1)n_p - m_p(n_s + n_q - 1) \right] \\ +(m_p n_r - m_r n_p)(m_s + m_q - 1)(m_p + m_r - 1) \end{array} \right] F(-4,-2) \\[12pt] + \left[ \begin{array}{l} n_r(n_r - 1)\left[ (m_s + m_q - 1)n_p - m_p(n_s + n_q - 1) \right] \\ +(m_p n_r - m_r n_p)(n_s + n_q - 1)(n_p + n_r - 1) \end{array} \right] F(-2,-4) \end{array} \right\}$$

$$C_{i,j,k,l}^{3} = m_r m_q \left\{ \begin{array}{l} (m_p n_s - m_s n_p)\left[ (m_r + m_q - 2)(m_p + m_s - 1) \right] \\ +m_s(m_s - 1)\left[ (m_r + m_q - 2)n_p - m_p(n_r + n_q) \right] \end{array} \right\} F(-5,-1)$$

$$+ \left\{ \begin{array}{l} m_r m_q \left( \begin{array}{l} (m_p n_s - m_s n_p)\left[ (n_r + n_q)(n_p + n_s - 1) \right] \\ +n_s(n_s - 1)\left[ (m_r + m_q - 2)n_p - m_p(n_r + n_q) \right] \end{array} \right) \\[12pt] +n_r n_q \left( \begin{array}{l} (m_p n_s - m_s n_p)\left[ (m_r + m_q)(m_p + m_s - 1) \right] \\ +m_s(m_s - 1)\left[ (m_r + m_q)n_p - m_p(n_r + n_q - 2) \right] \end{array} \right) \end{array} \right\} F(-3,-3)$$

$$+ n_r n_q \left\{ \begin{array}{l} (m_p n_s - m_s n_p)\left[ (n_r + n_q - 2)(n_p + n_s - 1) \right] \\ +n_s(n_s - 1)\left[ (m_r + m_q)n_p - m_p(n_r + n_q - 2) \right] \end{array} \right\} F(-1,-5)$$

$$C_{i,j,k,l}^{5} = \left[ -\left( m_r n_q - m_q n_r \right)\left( m_p n_s - m_s n_p \right) + \left( m_s n_q - m_q n_s \right)\left( m_p n_r - m_r n_p \right) \right] F(-2,-2)$$

$$C_{i,j,k,l}^{7} = -m_q \left\{ m_r \left( m_p n_s - m_s n_p \right) + \left( m_r n_p - m_p n_r \right)\left[ m_s + m_q - 1 \right] \right\} F(-3,-1)$$
$$-n_q \left\{ n_r \left( m_p n_s - m_s n_p \right) + \left( m_r n_p - m_p n_r \right)\left[ n_s + n_q - 1 \right] \right\} F(-1,-3)$$

$$C_{i,j,k,l}^{9} = -\left( m_r n_p - m_p n_r \right)\left( m_s n_q - m_q n_s \right) F(-2,-2)$$

$$C_{i,j,k,l}^{11} = -\left(m_s n_q - m_q n_s\right) \times \begin{bmatrix} m_p m_r \left(m_p - 1\right)\left(m_s + m_q - 1\right) F\left(-5,-1\right) \\ \begin{bmatrix} \left(n_p n_r \left(m_p + m_r\right) - m_p n_r (n_r - 1)\right)\left(m_s + m_q - 1\right) \\ + \left(m_p m_r \left(n_p + n_r\right) - n_p m_r (m_r - 1)\right)\left(n_s + n_q - 1\right) \end{bmatrix} F\left(-3,-3\right) \\ n_p n_r \left(n_p - 1\right)\left(n_s + n_q - 1\right) F\left(-1,-5\right) \end{bmatrix}$$

$$C_{i,j,k,l}^{13} = \begin{Bmatrix} -\left(m_p - 1\right) m_s m_p m_r m_q \left(m_r + m_q - 2\right) F\left(-6,0\right) \\ + \begin{Bmatrix} \left[(m_s - 1)n_r n_q - m_r m_q \left(n_p + n_s\right)\right] m_s m_p \left(n_r + n_q\right) \\ + \left[(n_s - n_p - 1)m_p - n_p m_s\right] n_s m_r m_q \left(m_r + m_q - 2\right) \\ + \left[(m_s - 1)n_p m_r m_q - n_r n_q m_p \left(m_p + m_s - 2\right)\right] m_s \left(m_r + m_q\right) \end{Bmatrix} F\left(-4,-2\right) \\ + \begin{Bmatrix} \left[(n_s - 1)m_r m_q - n_r n_q \left(m_p + m_s\right)\right] n_s n_p \left(m_r + m_q\right) \\ + \left[(m_s - m_p - 1)n_p - m_p n_s\right] m_s n_r n_q \left(n_r + n_q - 2\right) \\ \left[(n_s - 1)m_p n_r n_q - m_r m_q n_p \left(n_p + n_s - 2\right)\right] n_s \left(n_r + n_q\right) \end{Bmatrix} F\left(-2,-4\right) \\ -\left(n_p - 1\right) n_s n_p n_r n_q \left(n_r + n_q - 2\right) F\left(0,-6\right) \end{Bmatrix}$$

$$C_{i,j,k,l}^{15} = -\left(m_r n_q - m_q n_r\right)\left[m_p \left(m_p - 1\right) F\left(-3,-1\right) + n_p \left(n_p - 1\right) F\left(-1,-3\right)\right]$$

$$C_{i,j,k,l}^{17} = -m_p m_q \left[\left(m_q + m_s - 1\right)\left(m_p - 1\right)\right] F\left(-4,0\right) + n_p n_q \left[\left(n_q + n_s - 1\right)\left(n_p - 1\right)\right] F\left(0,-4\right)$$
$$+ \left\{n_p m_q \left[\left(m_q + m_s - 1\right)\left(n_p - 1\right)\right] + m_p n_q \left[\left(n_q + n_s - 1\right)\left(m_p - 1\right)\right]\right\} F\left(-2,-2\right)$$

$$U_{i,j,k,l}^{1} = -\left[m_p n_r - m_r n_p\right] \times \left[m_q \left(m_q - 1\right) F\left(-3,-1\right) + n_q \left(n_q - 1\right) F\left(-1,-3\right)\right]$$
$$U_{i,j,k,l}^{3} = \left(m_q n_r - m_r n_q\right) F\left(-1,-1\right)$$
$$U_{i,j,k,l}^{5} = \left(m_s n_r - m_r n_s\right) F\left(-1,-1\right)$$

**Bibliography**

[1] R. Gruber and J. Rappaz, *Finite Element Methods in Linear Ideal MHD*, Springer, 1985

[2] D. Schnack, D.C. Barnes, D.P. Brennan, et. al., "Computational modeling of fully ionized magnetized plasmas using the fluid approximation", Phys. Plasma 13 Art. No. 058103 (2006)

[3] S. C. Jardin, "A Triangular Finite Element with First-derivative Continuity Applied to Fusion MHD Applications", J. Comp. Phys, **200**, 133 (2004)

[4] S. C. Jardin and J. A. Breslau, "Implicit solution of the four-field extended-magnetohydrodynamic equations using high-order high-continuity finite elements", Phys. Plasma, **12**, 056101 (2005)

[5]  C. R. Sovinec, A. H. Glasser, G. A. Gianakon et al., J. Comput. Phys. **195**, 355 (2004).

[6] L. Chacon, D. A. Knoll, and J. M. Finn, "Implicit, nonlinear reduced resistive MHD nonlinear solver", J. Comput. Phys, **178**, no 1, pp. 15-36, 2002

[7] L. Chacon and D. A. Knoll, "A 2D high-beta Hall MHD implicit nonlinear solver", J. Comput. Phys, **188**, no 2, pp. 573-592, 2003

[8] A. H. Glasser and X. Z. Tang, "The SEL macroscopic modeling code", Computer Physics Communications **164** p237 (2004)

[9] G. Strang and G. Fix, *An analysis of the Finite Element Method*, Prentice-Hall, N.J., 1973

[10] O. C. Zienkiewicz, *The Finite Element Method*, 3rd edn, McGraw-Hill, London, 1977]

[11] M. Zlamal, "Some recent advances in the mathematics of finite elements', in *The Mathematics of Finite Elements and Applications* (J. R. Whiteman, Ed.), Academic Press, 1973, pp. 59-79.

[12] L. D. Landau and E. M. Lifschitz, *Fluid Mechanics*, Addison-Wesley, Reading, Mass. (1959)

[13] N. Ferraro and S. C. Jardin, "Finite element implementation of Braginskii's gyroviscous stress with application to the gravitational instability", Phys. Plasmas **13**: No. 092101 2006

[14] W. Park, E. V. Belova, G. Y. Fu, et al., Phys. Plasmas **6** (1999) 1796-1803 (Part 2)

[15] I. N. Molchanov and L. D. Nikolenko, "On an approach to Integrating Boundary Problems with a non-unique solution", Information Processing Letters **1** (1972) 168-172

[16] R. L. Richard, R. D. Sydora, and M. Ashour-Abdalla, "Magnetic reconnection driven by current repulsion", Phys. Fluids B **2**, 488 (1990)

[17] J. Birn, J. F. Drake, M. A. Shay, *et al.*, J. Geophys. Res., [Space Phys.] **106**, 3715 (2001)

[18] J. Breslau and S. C. Jardin, Phys. Plasmas **10** p. 1291 (2003)

[19] J. W. Demmel, J. R. Gilbert, and Y. S. Li, SUOERLU: Users Guide, U. C. Berkeley, 2003.